



Simulation of accumulation of contact fatigue damages in railway wheels

User's manual

2013

Contents

| | |
|--|--------------|
| 25. ROLLING CONTACT FATIGUE..... | 25-3 |
| 25.1. GENERAL INFORMATION..... | 25-3 |
| 25.2. ROLLING CONTACT FATIGUE | 25-5 |
| 25.2.1. Contact fatigue damages of the railway wheels | 25-5 |
| 25.2.2. Reduced stress criterion | 25-6 |
| 25.2.3. Contact fatigue curve of wheel steel | 25-8 |
| 25.2.4. Accumulation of contact fatigue damages | 25-10 |
| 25.3. CONTACT PROBLEM | 25-12 |
| 25.3.1. Methods for decrease of computer time for solution of contact problems | 25-12 |
| 25.3.2. Finite element fragments on elastic foundation | 25-14 |
| 25.3.3. Fast algorithm for solving contact problem | 25-16 |
| 25.3.3.1. Algorithm for definition of the maximum pressure in the contact area | 25-17 |
| 25.3.3.2. Algorithm for solution of the normal contact problem | 25-19 |
| 25.3.3.3. Algorithm for solution of tangential contact rolling problem | 25-24 |
| 25.4. MODELING ACCUMULATION OF CONTACT FATIGUE DAMAGE IN UM RCF MODULE.. | 25-28 |
| 25.4.1. Input data | 25-28 |
| 25.4.2. Creation of finite element mesh of the wheel | 25-29 |
| 25.4.3. Definition of contact forces by using fast algorithm | 25-30 |
| 25.4.4. Definition of stresses in area of wheel and rail contact..... | 25-31 |
| 25.4.5. Damages accumulation in nodes of finite element mesh | 25-33 |
| 25.4.6. Consideration of wear of the wheel profile | 25-33 |
| 25.5. WORKING WITH UM RCF MODULE..... | 25-34 |
| 25.5.1. Running UM RCF module | 25-34 |
| 25.5.2. Interface of the module | 25-35 |
| 25.5.3. Overview of the buttons on the "Design Scheme" toolbar..... | 25-36 |
| 25.5.4. Parameters..... | 25-37 |
| 25.5.4.1. The «Calculation» tab | 25-38 |
| 25.5.4.2. The «Material» tab | 25-40 |
| 25.5.4.3. The «Visualization» tab | 25-41 |
| 25.5.5. Imaging modes..... | 25-41 |
| 25.5.5.1. Mesh | 25-42 |
| 25.5.5.2. Coloring | 25-42 |
| 25.5.5.3. Isolines..... | 25-42 |
| 25.5.5.4. Maximum damage | 25-43 |
| 25.5.5.5. Numbers of nodes | 25-43 |
| 25.5.6. Performing calculation | 25-43 |
| 25.5.7. Viewing the results of calculation..... | 25-46 |
| 25.5.8. Saving the results of calculation | 25-47 |
| 25.5.9. Deleting the results of calculation..... | 25-47 |
| 25.5.10. Samples | 25-47 |
| REFERENCES..... | 25-49 |

25. Rolling Contact Fatigue

25.1. General information

Program package **Universal Mechanism (UM)** has been developed at the Laboratory of Computational Mechanics of Bryansk State Technical University.

Module **UM Rolling Contact Fatigue (RCF)** represents additional program tool integrated in **UM Simulation** program. The indication of presence of the module in current configuration of UM is sign «+» in the corresponding line of **About** window (command menu **Help | About program...**), figure 25.1.



Figure 25.1. List of modules in **About program** window

Module **UM RCF** is developed for simulation of accumulation of contact fatigue damages in railway wheels. The module may be used for implementing of multivariant comparative calculations, for example for solution of the problem of the wheel tread profile optimization according to a contact fatigue criterion.

UM RCF allows the user:

- to define the velocity of accumulation of contact fatigue damages in wheels with the different tread surfaces by using the data which are obtained by simulation of railway vehicle dynamics by means of the **UM Loco**;
- to take into account wheel profile wear-out effect on the rate of accumulation of contact fatigue damages (module **UM Wheel\Rail Wear**);
- to represent processes of the stress modeling and the damage accumulation in the wheel with the help of graphic interface including isolines and coloring.

For modeling processes of contact fatigue damages accumulation in **UM RCF** the following assumptions are used.

- The materials of the contacting bodies are uniform, isotropic and elastic.
- Geometric forms of contact surfaces exert determinative influence on conditions in contact, and these conditions depend from structural forms of wheels weakly.
- The temperature level arising in a wheel does not influence on a stress state and mechanical properties of wheel material considerably.

UM RCF requires the **UM Loco** module. For taking into account the influence of wheel profile wear on rate of contact fatigue damages accumulation, module **UM Wheel\Rail Wear** is also necessary.

This manual is compiled as follows. Practical issues are discussed in Sect. 25.5. The description of the algorithms involved in the program is considered in Sect. 25.4. More information about contact fatigue and methods of solution of the contact problem can be obtained in Sect. 25.2 and 25.3.

25.2. Rolling contact fatigue

Contact fatigue causes some widespread defects of machine elements. Interaction of wheel and rail is characterized by the following features. It is firstly a very high pressure (more than 1000 MPa) that causes plastic deformation of subsurface layers under big friction coefficients. Rolling of a wheel along a rail, especially at moving in curve sections, is accompanied by considerable longitudinal and lateral creeps that exerts large damaging effect. Besides, cases of full sliding of wheel along rail are possible under braking. It results in thermomechanical damages of rolling surface and rather fast spalling of surface damaged layers under acting of contact stresses. Due to high levels of contact stress and temperature arising on frictional surfaces of wheel cracks appear. The cracks are typically either parallel or perpendicular to the wheel tread. With continued rolling the cracks grow and when the material is weakened to the point of failure, the spalls are formed. A network of cracks may progress into rolling contact fatigue shells [1].

25.2.1. Contact fatigue damages of the railway wheels

Surface contact fatigue damages (figure 25.2a) become apparent as inclined parallel cracks placed on the rolling circle and spalles from them. This type of defect is named thread checks (word for word – bursting of the rolling surface). At the first stage hair-like cracks inclined about under equal angles to generatrix of the wheel cylindrical surface appear on the rolling surface. Angle of inclination of the cracks in different cases may change from 20 – 30 to 45 degrees. Section where such cracks are discovered may be situated at 25 – 40 mm from outside wheel face, on the middle of tread, in the area adjoining to flange. Within process of increasing of run small cracks begin to unite forming local spalles. Later local spalles may generate chain of entire spalles which are objectionable defect and the wheel is liable to turning [2].

Subsurface contact fatigue damages (figure 25.2b) appear at depth 3 – 6 mm and more and cracks commonly develop towards tread causing spalling in form of shells. However crack may develop inside of wheel that, in case of many times turned rim, under action of impact load may result in destruction of wheel [3].



a)



b)

Figure 25.2. Contact fatigue damages of railway wheel: a) shallow; b) subsurface

Spectrum of forces dependent from wheel load, position of wheel on rail, wheel and rail profiles, friction forces acts on the wheel tread. Unfavorable combination of worn wheel and rail profiles at some positions of wheel on rail is the factor which contributes to arising normal and tangential stresses and thus to arising rate of damages accumulation, as pointed out in [2].

One of features of appearing subsurface contact fatigue damages of wheel is that rim material under action of normal and tangential forces is in complicated stress state when directions of main stresses change during cycle and stress components reach maximum values at one time [4].

In case of rolling with sliding under relatively small friction coefficient the maximum tangential stresses causing plastic flow of material is located at depth determined by dimension of contact ellipse semiaxis. The power law [2] is used for the simulation of damages accumulation. It is based on the condition that rate of fatigue damages accumulation is connected with amplitude value of maximum tangential stress at the considered point. Parameters of the dependence are obtained experimentally. It is supposed that linear hypothesis of damages accumulation is applicable.

Mostly subsurface damages develop in the presence of inclusions (interstices, blowholes) as well as of heterogeneities of structure. Modeling of plasto-elastic stress state using finite element method shows [5] that local stresses increase in the area close to the defect and as a result the plastic deformation has place. It causes residual stresses that may be tensile ones. It helps rising the crack [2].

However contact fatigue damages may arise in absence of evident material defects [6] at depth about 4 mm from tread where the reduced stresses reach maximum value exceeding the fatigue range of material in at the considered point. Such damages arise under large stresses in cases of unfavorable combination of worn wheel and rail profiles especially of channel-shaped profile of wear [2], when normal stresses under wheel load 120 kN arise from 1100 to 2300 MPa and more. Contact stresses arise also at decreasing wheel diameter after repeated wheel turning.

25.2.2. Reduced stress criterion

One of the models that is applied for analysis of fatigue in rolling contact (RCF) at railway transport is so-called *Shakedown Diagram Model*. It is guided by shakedown theory of wheel material [7]. Another approach is based on the *Dang Van fatigue criterion based model*. Both approaches take into account the next demands. Firstly, to account the multi-axial stress field induced in the material by the applied forces. Secondly, railway engineers need a rapid and sufficiently accurate tool in what had been implemented regardless of the vehicle dynamic software providing time-history of normal and tangential wheel/rail contact interaction $P(t)$, $Q(t)$. These models are based on different assumptions and reduced stress criteria.

According to criterion based on the Dang Van's criterion [8], damage occurs if the combination of the value $\tau_a(t)$ of tangential stress in the most dangerous shear plane and the value $\sigma_h(t)$ of the hydrostatic stress at the considered material point fulfils one or both of following two inequalities during some time portion $t_1 < t < t_2$ of the full stress cycle

$$\begin{aligned} \tau_{EQ1} &= \tau_a(t) + a_{DV} \sigma_h(t) > \tau_e, & (a) \\ \tau_{EQ2} &= \tau_a(t) - a_{DV} \sigma_h(t) < -\tau_e, & (b) \end{aligned} \quad (25.1)$$

where $\tau_a(t)$ is the time-dependent value of the shear stress at the specified material point and in the specified shear plane through this point. The value $\tau_a(t)$, called shear stress amplitude is calculated as the difference between the current magnitude at time t of the rotating shear stress in the specified plane and its mid magnitude during one cycle;

$\sigma_h(t)$ is the time-dependent value of the hydrostatic stress at the same material point, positive when tensile;

τ_e is the material parameter usually taken equal to the fatigue limit of the material in pure shear, positive;

a_{DV} is a dimensionless material parameter representing the influence of the hydrostatic stress, positive.

Criteria (figure 25.1a, b) are illustrated in figure 25.3. Since the critical shear plane is unknown, the fulfillment of the criterion must be examined for all possible shear planes through each considered point of material. In order to reduce the CPU efforts, instead of the shear stress in a specified plane, the largest shear stress in a material point i.e. the Tresca shear stress may be used

$$\tau_{Tresca}(t) = [\sigma_1(t) - \sigma_3(t)]/2,$$

where σ_1, σ_3 are algebraic largest and least main stress correspondingly.

Using the amplitude of the Tresca shear stress a simplified fatigue criterion is defined as

$$\tau_{EQ3} = \tau_{a,Tresca}(t) + a_{DV}\sigma_h(t) > \tau_e \quad (25.2)$$

The damage calculated by criterion (25.2) is a scalar quantity. Only the largest damage in a material point is identified and different shear planes are not considered.

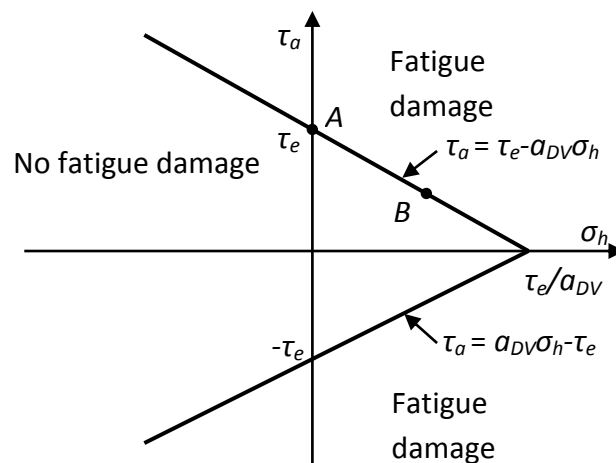


Figure 25.3. Dang Van diagram of cyclical fatigue for uniaxial fatigue damage

25.2.3. Contact fatigue curve of wheel steel

The wheels of freight cars in the Russian Federation are produced of the Steel 2 (GOST 10791-89), with following chemical composition.

| Element | Carbon | Manganese | Silicon | Phosphorus | Sulfur |
|--------------------------|-----------|-----------|-----------|-------------------|-------------------|
| Element mass fraction, % | 0,55–0,65 | 0,50–0,90 | 0,22–0,45 | No more than 0,04 | No more than 0,04 |

It is allowed content of nickel, chrome and copper no more than 0,25% of each. The wheel steel has following mechanical properties:

| | |
|--|-------------|
| Ultimate strength, MPa | 911 – 1107 |
| Elongation, % | No less 8 |
| Reduction of area, % | No less 14 |
| Brinell hardness number at depth 30 mm | No less 255 |
| Impact resistance at temperature 20°C, Joule/centimeter ² | More 0,20 |

Yield stress and contact fatigue strength of the wheel steel are not specified in GOST.

One of the difficult problems is experimental definition of characteristics of contact fatigue strength of the wheel steels. In work [2], an approximate estimation of limit of contact fatigue endurance of the wheel steel is given. This estimation is indirect. It corresponds to the maximum contact pressure after Hertz 1000 MPa. The interaction of wheel and rail is characterized by forces arising maximum contact pressure exceeding this value. It is advisable that the method for calculation of contact fatigue strength of wheel should create so as accumulation of fatigue damages would be registered in points of material of surface layer. For that it is convenient to use meshes in nodes of which the damages would be calculated.

Using the finite element meshes ensures favorable conditions for the definition of stresses and by means of stresses to calculate the damages in the nodes. Assumptions concerning the form of the contact patch and distribution of forces on the contact surface fall away. A curve of contact fatigue strength of wheel steel is necessary for realization of such approach. The curve allows defining number of variable stress cycles until fracture depending on criterion characterizing stress state in the contact area occurs. Maximum tangential stress is considered as such criterion in many papers.

In papers [3] and [9] the results of testing the wheel steels on contact fatigue strength are presented. The testing carried out using simulation machine designed by VNIIZhT (All-Russian Railway Research Institute) according to the scheme of rolling of cylindrical rollers with diameter 40 mm produced of the wheel steel on the toroidal rollers produced of hard alloy VK8 of diameter 42 mm with curvature radius of torus generatrix 12 mm. The maximum Hertz pressure calculated on the assumption that deformations of material of specimens are elastic was accepted as a parameter characterizing stress state in the contact area. Numbers of variable stress cycles until fracture on five levels of loading and conditional maximum contact pressure corresponding to them are presented below:

| | | | | | |
|------------------------------------|-------|-------|-------|-------|-------|
| Loading, N | 119,3 | 226,4 | 495,1 | 749,4 | 988,6 |
| Maximum contact pressure, MPa | 1680 | 2080 | 2700 | 3100 | 3400 |
| Durability, number of circles·10-5 | 8,0 | 5,17 | 2,98 | 2,34 | 1,89 |

The presented pressures are relative as under least of above loading the plastic deformations are observed in the contact area. It changes the law of contact pressure distribution in comparison with the Hertz distribution and stress state in the contact area.

Using the results of this test in work [10] by means of numerical method, data for building the curve of contact fatigue strength of wheel steel on the assumption of elastic adaptability of specimen material were obtained. The first loading of the specimen with force of the specified level is accompanied by elastic-plastic deformations while the material works at elastic deformations under following loadings. The rolling contact problem with taking into account elastic-plastic deformations of the specimen material of the wheel steel is solved by finite element method under the same physical-mechanical properties and geometrical characteristics as in the tests described above. The reduced stress based on Dang Van's criterion is accepted as parameter characterizing the stress state in the area of contact (par. 25.2.2):

$$\tau_{DV} = \tau_{\max}^a + a_{DV} \sigma_0, \tag{25.3}$$

where τ_{\max}^a is amplitude value of the maximum tangential stress in the point under consideration;

$$\sigma_0 = \frac{\sigma_1 + \sigma_2 + \sigma_3}{3}$$

is middle value of the hydrostatic stress at point;

$\sigma_1, \sigma_2, \sigma_3$ are main stresses at point.

The first item in equation (25.3) is the time-varying stresses causing damages of the specimen material on their certain level. Negative hydrostatic pressure, which characterizes for the points situated in the contact area, exerts restrictive influence on the damages accumulation process. Coefficient aDV is analogous with the material sensitivity index to asymmetry of variable stress cycle. Its value is accepted 0.1 depending on breaking point of specimen material [11].

The values of the obtained reduced stress appearing in dangerous points under the prescribed loadings are used for building the contact fatigue curve of wheel steel (figure 25.4). For the convenience of using of contact fatigue curve in calculations, it is approximated by the function

$$N = 2,603 \cdot 10^{11} \tau_{DV}^{-2,5}, \tag{25.4}$$

where N is number of cycles until fracture.

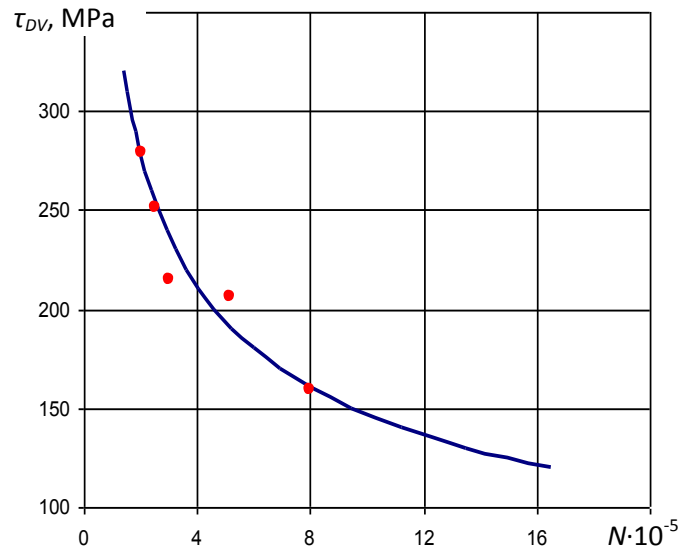


Figure 25.4. Curve of contact fatigue of the wheel steel

25.2.4. Accumulation of contact fatigue damages

In work [2] the model of accumulation of contact fatigue damages is based on positive not decreasing in time function $Q(M, t)$. This function characterizes damage degree of the material in a point $M(x, y, z)$, depending on amplitude value of the stress in the point. Fracture occurs when this function reaches the prescribed threshold value. For investigation of the damages accumulation in wheel material the model of linear summing is used. It supposes that damage increment does not depend on cumulative damage. For definition of rate of the fatigue damages accumulation, next equation is used

$$q(x, y, z, t) = \frac{\partial Q(x, y, z, t)}{\partial t} = c[\Delta\tau_1(x, y, z, t)]^m,$$

where c, m are constants defined experimentally;

$\Delta\tau_1(x, y, z, t)$ is difference between maximum and minimum value of maximum tangential stress in point with coordinates x, y, z during one cycle of loading.

Damages accumulated in point with coordinates x, y, z during N cycles is defined by expression

$$Q(x, y, z) = \int_0^N q(x, y, z, n)dn + Q_0(x, y, z),$$

where $Q_0(x, y, z)$ is distribution of the initial damage.

In the general case the condition of approaching of fracture is written as

$$\int_0^L c \sigma^m(x, y, z, n) dn + Q_0(x, y, z) = 1$$

where maximum tangential stress τ_1 or tension stress may be taken as σ ; L is the number of cycles until fracture.

25.3. Contact problem

Strength and wearing capacity of the details and assemblies of the machines are mainly defined by the contact conditions. Conception “solving of the contact problem” may include the definition of the following parameters: shape and size of a contact patch; normal and tangential forces at contact; the law of the distribution of contact pressure on contact surfaces; the distribution of stress in the area of contact. The *normal contact problem* is usually considered as the definition of distribution of contact forces between two solid bodies pressed along the common normal to the initial point of contact.

Analytical methods of solutions of contact problem supplies minimal timetable for solving the problems but their application is complicated if the contact surfaces have complex geometric forms and the bodies could not be represented by half-spaces.

Numerical methods allow to model contact stress without constraints connected with geometrical forms of body surfaces. However for obtaining the sufficient accuracy of solution it demands usage of design schemes of large dimension what leads to considerable computation time.

Fast algorithms ensure small computer time for solving the contact problems but use vastly simplified design scheme for the definition of shapes and sizes of contact patches and the laws of contact pressure distribution.

25.3.1. Methods for decrease of computer time for solution of contact problems

Contact surfaces of wheels and rails are worn out in service and obtain complicated geometrical forms. Most often for solution of such problems finite element (FE) models are applied in view of nonlinearity of such contact problems. The feature of the wheel and the rail contact is the localization of stresses in small volumes in comparison with the contact body sizes. Therefore fragments adjoining to the contact area are selected for the FE model of the wheel and the rail (figure 25.5a).

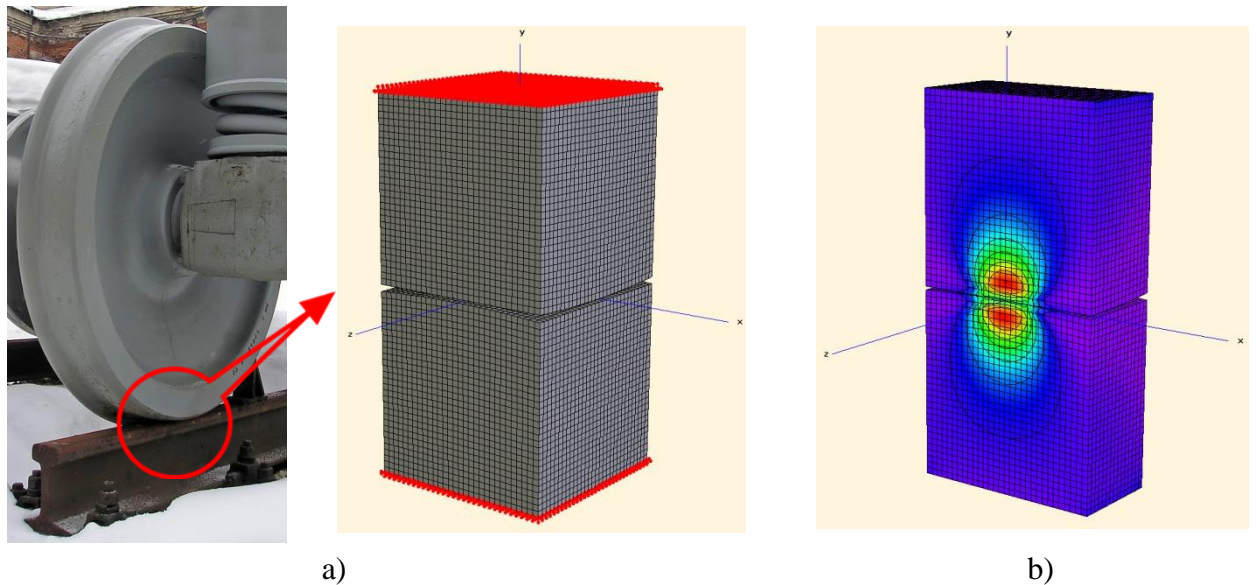


Figure 25.5. FE model of wheel and rail: a) selecting wheel and rail fragments for FE model; b) reduced stress isolines σ_{red}^{IV} in contact area

Selected fragments are divided into finite elements; rigid constraints are put on nodes of the FE model that forbid linear displacements and rotation of bodies. Results of solution of the problem in the form of reduced stress isolines σ_{red}^{IV} are shown in figure 25.5b.

However, including even relatively small fragments of bodies in FE model leads to large dimension, what demonstrates the example shown in figure 25.5. The presented FE model has the following parameters: sizes of wheel and rail fragments are $30 \times 30 \times 30$ mm, number of finite elements is 54000, number of nodes is 59582, number of degrees of freedom is 178746. The problem demands the solution of system with big number of algebraic equations that results in significant computation time – even using a modern computer it is needed several minutes for solution of such problem. For modeling of contact fatigue accumulation it is necessary to solve contact problem many times – tens of thousand times, therefore one of important problem is decreasing CPU time for its solution.

It is possible to decrease number of finite elements of model by applying rough meshes far from a contact and mesh refinement close to it. In work [12] transition element obtained on the basis of finite element with eight nodes is applied. Eight tetrahedrons, four elements with six nodes and one element with eight nodes enter in its structure (figure 25.6). It allows the transformation from one big element to nine small elements. Difficulties with its applying arise at mesh refinement along three directions.

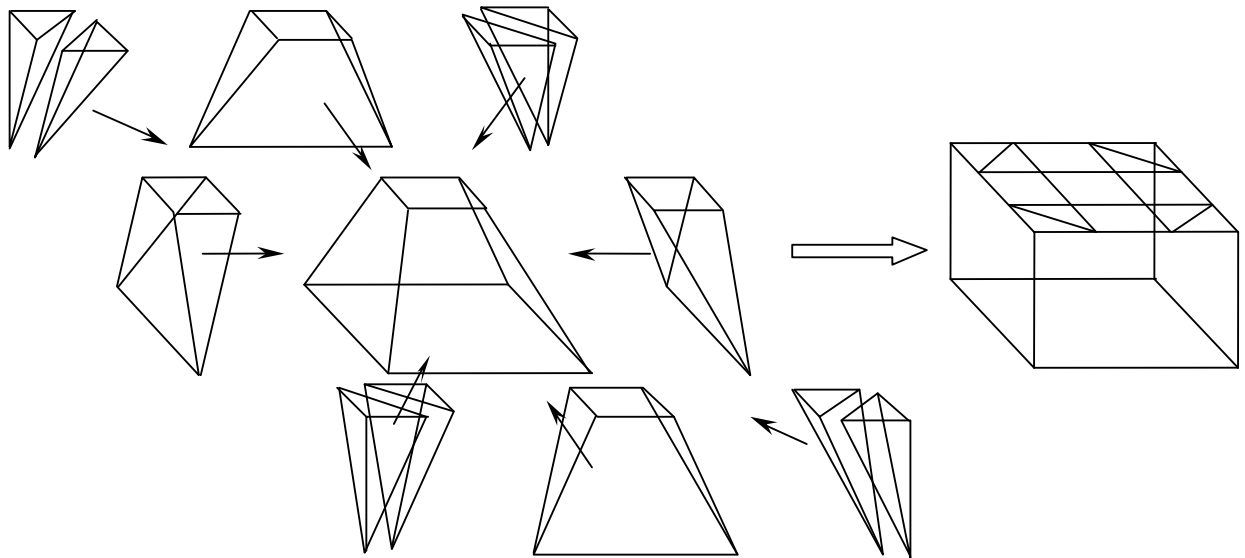


Figure 25.6. The transition element used to grind a finite element mesh

To decrease the dimension of finite element scheme, a method of reducing of nodes is proposed in work [13] and method of super cells is used in work [14]. As the number of dimension of finite element scheme is decreased, the number of dimension of algebraic equations set is reduced but the equations become very cumbersome that may result in increasing of computation time. Moreover the above methods of reducing the dimension of FE-mesh are not universal.

25.3.2. Finite element fragments on elastic foundation

The following approach for solving contact problem is proposed in [15]. Small three-dimensional fragments of the wheel and the rail adjacent to contact area are chosen. The chosen fragment is divided into eight node finite elements of serendipity finite element family [16] and is put on elastic foundation. Node displacements, distribution of pressure and forces in contact are defined using the method of node iterations [17]. The stiffness of the elastic foundation that ensure correct solution of the contact problems with using the finite element fragments of small thickness is defined by analytic and numerical methods.

The method was tested by contact problem for two steel cylinders of 0.2 m radii with skew axes pressed together by the force of 100 kN (figure 25.7).

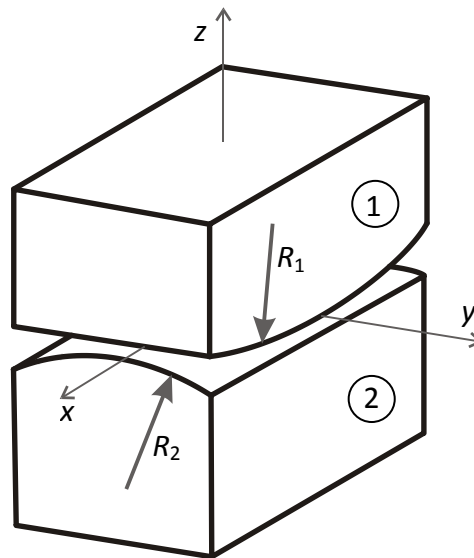


Figure 25.7. Fragments of cylinders

The Hertz solution gives contact patch radius of 5.2 mm and maximum pressure p_0 of 1766 MPa. The problem was solved by using the FE model of large dimension with 59582 nodes and 54000 finite elements and also the fragments on the elastic foundation with 10, 5 and 1 layers of the finite elements. In all FE models the length of ribs of finite elements was taken equal 1 mm. Results of solution are presented in the form of the contact pressure distribution p in figure 25.8 and in table 25.1.

Applying the finite element fragments on the elastic foundation allows essentially decreasing CPU expenses along with sufficient accuracy of definition of the contact patch dimensions and maximum pressure. figure 25.8a, figure 25.8b give the isolines of equivalent von Mises stresses in the plane xy . They are analogous for the large scheme and the fragment with 5 layers. In the first case equivalent von Mises stress in the most strained node placed in depth of 2 mm runs up to 1147 MPa and in the second one to 1155 MPa. The finite element scheme consisting of one layer ensures sufficient exactness of the determination of maximum pressure in contact (figure 25.8c).

Table 25.1

Results of solution of test using finite element fragments on the elastic foundation

| Design scheme | Number of finite elements | Radius of contact patch, mm (error) | Maximum pressure, MPa (error) | Computer time, s |
|---------------------------------|---------------------------|-------------------------------------|-------------------------------|------------------|
| Large finite element scheme | 54000 | 5,2 (0,38%) | 1758 (0,45%) | 670 |
| 10 layers on elastic foundation | 18000 | 5,17 (0,58%) | 1779 (0,74%) | 102 |
| 5 layers on elastic foundation | 9000 | 5,16 (0,77%) | 1745 (1,2%) | 46 |
| 1 layer on elastic foun- | 1800 | 5,51 (5,96%) | 1603 (9,2%) | 7 |

| | | | | |
|--------|--|--|--|--|
| dition | | | | |
|--------|--|--|--|--|

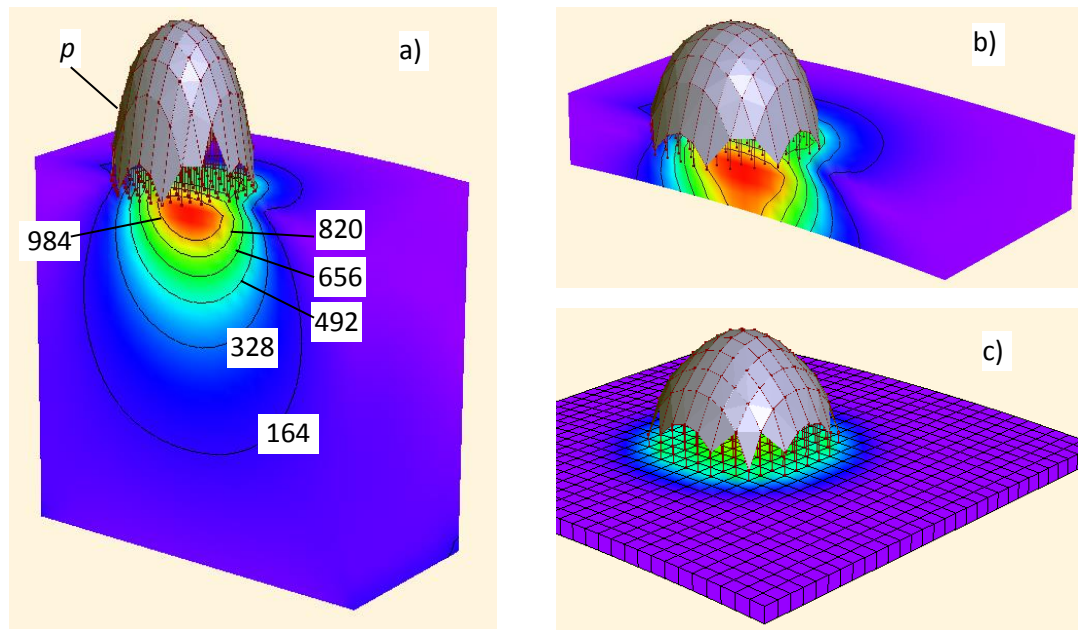


Figure 25.8. Distribution of the contact pressure p and isolines of the equivalent stresses σ_{eqv}^{IV} in the area of contact (MPa): a) large finite element scheme; b) five layers on the elastic foundation; c) one layer on the elastic foundation.

25.3.3. Fast algorithm for solving contact problem

The most widely used algorithm for solving of normal contact problem was proposed by W. Kik and J. Piotrowski [18]. Another one for solving of tangential contact rolling problem – the FASTSIM algorithm – was proposed by J. Kalker proposed [19].

In the process of wearing of wheels and rails the profiles of their surfaces become similar in shapes (so called conformal). The conformal or multipoint contact between them is possible, for which a fast algorithms [18] not always may be applied. This is typical for curve track sections. The *conformal* is named contact between two bodies that have the same surface profiles of considerable length. In this case, the contact patch is a spatial surface, which is not a plane. Examples of conformal and multipoint contacts are shown in figure 25.9.

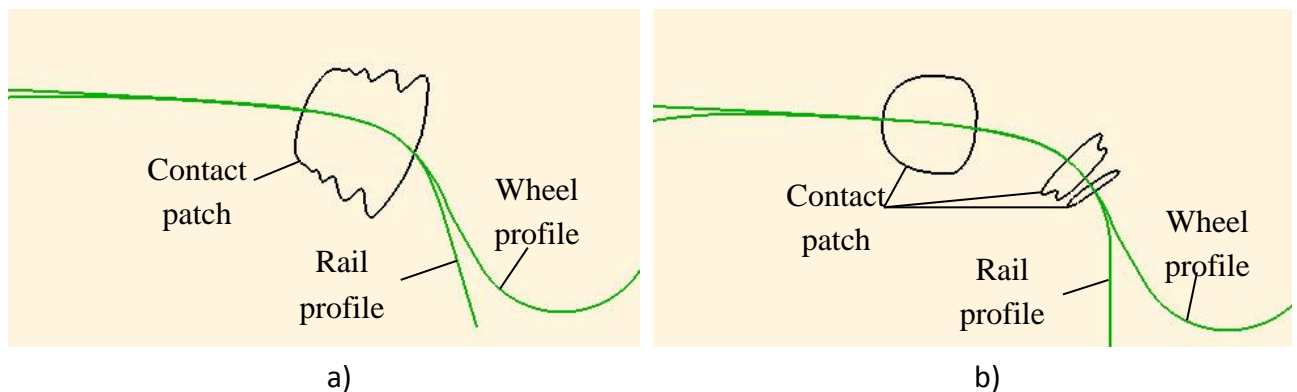


Figure 25.9. The contact between wheel and rail: a) conformal; b) multipoint

In the **UM RCF** module, a fast algorithm for solving the contact problem, which allows taking into account any type of contact including conformal and multipoint, is implemented. The description of this algorithm is given below.

25.3.3.1. Algorithm for definition of the maximum pressure in the contact area

The opportunity to simplify the procedure of the definition of the maximum pressure and the normal force in the contact may be discovered at examination of the solution of the contact problem for two spheres. For the spheres of radii R_1 and R_2 with Poisson's ratio of 0.3 the radius of contact is defined using expression [20]

$$a = 1,1093 \sqrt[3]{\frac{N}{E} \frac{R_1 R_2}{R_1 + R_2}}, \quad (25.5)$$

and the interpenetration of the bodies is equal

$$\delta = 1,233 \sqrt[3]{\frac{N^2}{E^2} \frac{R_1 + R_2}{R_1 R_2}}. \quad (25.6)$$

Solving jointly the equations (25.5) and (25.6) we will have

$$\delta = 1,36 \frac{N}{Ea}.$$

With using the obtained equation and expression for the maximum pressure in the contact

$$p_0 = \frac{3}{2} \frac{N}{\pi a^2},$$

we will find

$$p_0 = k_p \frac{E\delta}{a}, \quad (25.7)$$

where $k_p = 0,35$.

The Hertzian solution supposes elliptical contact patch. The interpenetration of the bodies is defined using the expression [21]

$$\delta = \frac{P_0}{E} b K(e),$$

where b is small semiaxis of the contact ellipse;

$K(e)$ is complete elliptic integral of argument e ,

$$e = \sqrt{1 - \beta^2}; \quad \beta = b/a;$$

a is the bigger semiaxis of the contact ellipse.

The shape and dimensions of the contact patch are defined by assigning the interpenetration $\delta_0 = K_B \delta$ of the surface of one body into other one. It is assumed that the line of intersection of the surfaces of the bodies is the patch contour. Then for the determination of the maximum pressure in Hertzian contact instead of expression (25.7) it is convenient to use

$$p_0 = \frac{k_p}{K_B} \frac{E \delta_0}{b} \tag{25.8}$$

In the result of wear, the surfaces of the wheels and the rails obtain complicated geometric shapes and the application of them in analytical calculations is difficult. For this reason, the finite element calculation schemes are widely used for the solution of the contact problems. The sufficient precision is ensured by refinement of the finite element mesh within the contact area. Some rather small fragments of wheel and rail adjacent to the contact area can be taken for the solution due to the localization of strains and stresses in comparatively small area (par. 25.3.2). Such types of fragments are used for the determination of the coefficients k_p and K_B .

The contact of two steel cylinders with orthogonal axes is considered. The radius R_2 of one of them is assumed to be 200 mm and the radius R_1 of another was varied in range from 200 to 2500 mm. The fragments of dimensions 40×30×50 mm along the axes O_x, O_y, O_z correspondingly are taken out from the cylinders (figure 25.7). Values of the elasticity constants for the materials of the cylinders are assumed equal: Young's modulus $E = 2 \cdot 10^{11}$ Pa, Poisson's ratio $\mu = 0.25$. The size of hexahedral finite element in the area of assumed contact is 0.5 mm. Displacements δ along the axis z were assigned for the nodes of the fragment 1 placed at the upper plane. The displacement was selected so as the normal force N in the contact was equal to 100 kN. The results of solution by using finite element method are presented in table **Ошибка! Источник ссылки не найден.**

Interpenetration $\delta_0 = K_B \delta$ of the body 1 surface was assigned at the definition of the contact area by using the fast algorithm. The value of the coefficient K_B was chosen so as the square of the contact area would be equal to the square of the Hertzian contact πab because the elliptical contact patch obtained by using the fast algorithm is not similar to Hertzian contact patch. Coefficient k_p was determined using the dependence

$$k_p = \frac{p_0 b}{E \delta} \tag{25.9}$$

Values of the coefficients K_B and k_p depending on the ratio β of smaller semiaxis b to greater semiaxis a are shown in table 25.2.

Table 25.2

Parameters of the contact of the two cylinders and value of the coefficients K_B and k_p under $N = 100$ kN, $R_2 = 200$ mm

| | | | | | | | | |
|---------------------------|-------|-------|-------|------|-------|--------|--------|--------|
| Radius R_1 , mm | 200 | 300 | 400 | 600 | 1000 | 1400 | 1800 | 2500 |
| Penetration δ , mm | 0,125 | 0,115 | 0,109 | 0,1 | 0,089 | 0,0824 | 0,0775 | 0,0715 |
| Maximum pressure | 1776 | 1556 | 1429 | 1274 | 1116 | 1028 | 969 | 902 |

| | | | | | | | | | |
|-----------------------|-------|-------|-------|-------|-------|-------|-------|-------|-------|
| p0, MPa | | | | | | | | | |
| Length of semiaxis | a, mm | 5,15 | 6,26 | 7,22 | 9 | 11,09 | 13 | 14,17 | 16,15 |
| | b, mm | 5,15 | 5 | 4,5 | 4,19 | 4,02 | 3,55 | 3,35 | 3,18 |
| β | | 1 | 0,8 | 0,62 | 0,47 | 0,36 | 0,27 | 0,24 | 0,2 |
| KB | | 0,53 | 0,556 | 0,528 | 0,544 | 0,56 | 0,53 | 0,51 | 0,508 |
| kp | | 0,366 | 0,338 | 0,295 | 0,267 | 0,252 | 0,221 | 0,209 | 0,2 |

The obtained results allows to accept the penetrate coefficient equal to 0.53 and recommend to use the following approximate expression for determination of the coefficient k_p

$$k_p = 0,146 + 0,294\beta - 0,073\beta^2 \tag{25.10}$$

The coefficients K_B and k_p are equal to 0.508 and 0.2 correspondingly if one dimension of the contact patch is noticeably greater than another one, that is typical for conformal contact or contact patch that is strongly elongated in the rolling direction.

25.3.3.2. Algorithm for solution of the normal contact problem

For the solution of the contact problem for wheel and rail the following data, obtained at modeling of dynamics of railway vehicle, are used: coordinates of the points of initial contact placed on the wheel and rail profiles, angle of rotation of wheel around longitudinal axis of rail, values of normal contact forces, longitudinal and lateral creep.

Let profiles of surfaces of wheel f_w and rail f_r be close or coincide on some section. The conformal or multipoint contact is possible between them. Let us consider the common case when opposite points a and b placed on the profiles of the wheel and rail surfaces do not coincide but may enter in contact at pressure of the wheel to the rail (figure 25.10).

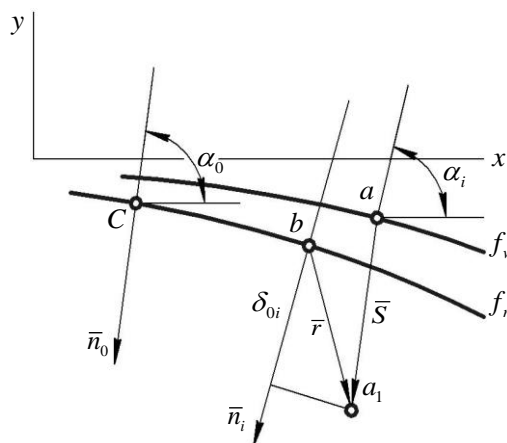


Figure 25.10. Definition of penetration of point

Let the penetration δ_0 of profile of the wheel surface to the surface of the rail occur in the direction of normal $\bar{n}_0 = \{x_0; y_0; z_0\}$, passing through the point of the initial contact C . The normal

When $\delta_{0i} > 0$ point i is penetrated under the rail surface.

The half of the length of the strip i is defined from condition

$$\xi^2 + (\xi - R_i)^2 = R_i^2, \quad (25.11)$$

where $R_i = r_i / \sin \alpha_i$ is the principal radius of curvature of the wheel surface in the point i;

r_i is radius of the circle on which the point i is placed;

α_i is angle of inclination of normal drawn through the point i.

Neglecting item ξ^2 in equation (25.11) and supposing $\xi = \delta_{0i}$, $x = x_{li}$, we will have

$$x_{li} = \sqrt{2R_i \delta_{0i}}. \quad (25.12)$$

Points placed on front and rear edges of the strips define the shape and dimensions of the contact patch.

Let us assume that pressure along a strip i is distributed by elliptic law

$$p = p_{0i} \sqrt{1 - \frac{z^2}{x_{li}^2}}, \quad (25.13)$$

where maximum pressure at middle of the strip i is defined from equation (25.8)

$$p_{0i} = \frac{k_p}{K_B} \frac{E \delta_{0i}}{x_{li}}.$$

The coefficient k_p may be calculated using equation (25.10). The half of length of the longest strip x_{li} and half of the size of the contact along the rail profile $\sum \Delta s_i / 2$ may be taken as semi-axes of the contact patch. Coefficient β is equal to the ratio of smaller and greater semiaxis.

Resultant of the pressure applied to strip i and its components are equal to

$$\Delta N_i = \frac{\pi}{2} p_{0i} x_{li} \Delta s_i, \quad \Delta P_i = \Delta N_i \sin \alpha_i, \quad \Delta Q_i = \Delta N_i \cos \alpha_i. \quad (25.14)$$

Let us consider the forces acting on rail. The obtained system of forces may be reduced to the only resultant force \bar{N} (figure 25.12a). When transfer the force $\Delta \bar{N}_i$ to the origin of coordinates, we obtain the force $\Delta \bar{N}_i$ that is applied to the origin of coordinates and adjoint moment ΔM_i (figure 25.12b). The system of forces is the concurrent one. Their sum gives resultant vector \bar{N} . The vertical, lateral and normal contact forces are defined by simple summation

$$P = \sum_{i=1}^n \Delta P_i, \quad Q = \sum_{i=1}^n \Delta Q_i, \quad N = \sqrt{P^2 + Q^2}. \quad (25.15)$$

Summing the adjoint moments we obtain the resultant moment MO

$$M_o = \sum_{i=1}^n \Delta P_i x_i - \sum_{i=1}^n \Delta Q_i y_i ,$$

where x_i, y_i are coordinates of the point placed on the rail profile on the middle of the strip i .

The resultant vector and the resultant moment are reduced to alone resultant force \bar{N} acting along the line equation of which is

$$y = kx + b , \tag{25.16}$$

where $k = \text{tg} \alpha_0 = P/Q$;

$$b = -h(\text{tg} \alpha_0 \sin \alpha_0 + \cos \alpha_0) ,$$

$$h = M_o / N .$$

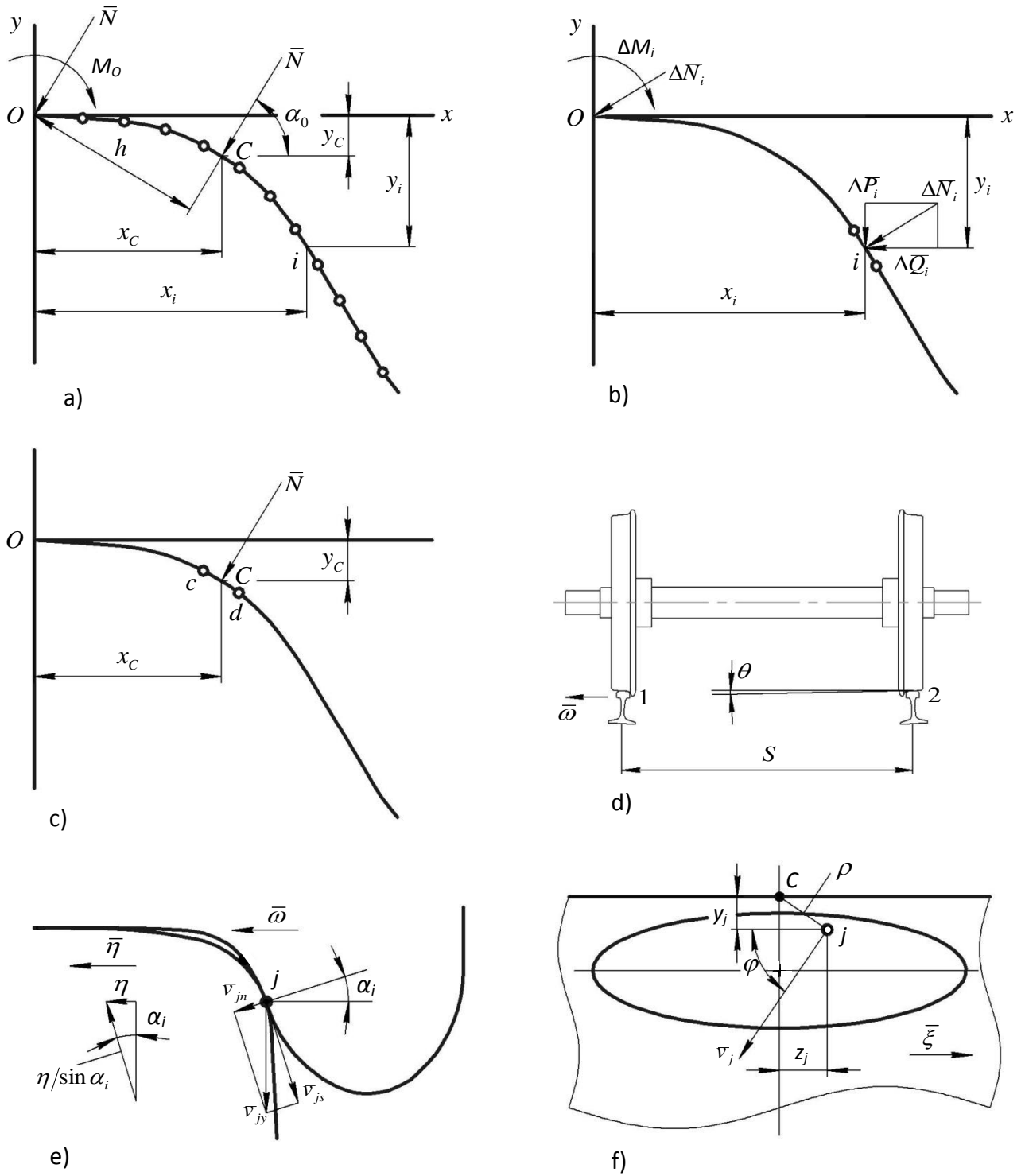


Figure 25.12. Definition of tangential stresses on contact surface

In order to define coordinates of the point C of application of the resultant \bar{N} , the rail profile is approximated by the line segments. The lines connecting two adjacent points are considered sequentially. The coordinates of the point of intersection of the line described by (25.16) and line passing through points c and d (figure 25.12c)

$$y = k_i x + b_i,$$

where $k_i = (y_c - y_d)/(x_c - x_d)$; $b_i = y_c - k_i x_c$.

If the coordinates of this point

$$x_C = (b - b_i)/(k_i - k); \quad y_C = k_i x_N + b_i$$

define the point placed within the segment cd, it is the point of application of the resultant \bar{N} .

In the case of multipoint contact, the considered procedure is applied for every patch. The division the contact patch into strips is not performed in the next cases: spatial curvilinear geometry of the patch appears not strongly and it may be replaced by equivalent Hertzian contact, the patch is strongly elongated in the rolling direction. In these cases the maximum pressure is defined by using the equation (25.8) and the normal force is equal to

$$N = \frac{2}{3} p_0 \pi a b$$

25.3.3.3. Algorithm for solution of tangential contact rolling problem

For solution of the tangential contact rolling problem (the definition of distribution of the tangential forces on a contact surface) the algorithm FASTSIM [19] is applied.

For determination of the compliance coefficient L , algorithm FASTSIM uses the ratio of the semiaxes of the elliptic contact patch

$$\beta = a / b,$$

where a is semiaxes of the ellipse taken along the rolling direction;

b is semiaxes of the ellipse oriented across the rolling direction.

The dimension of the longest strip is accepted as $2a$ and the dimension of the contact patch along the rail profile is set as $2b$.

The compliance parameter is defined by means of the equation

$$L = (|\xi|L_1 + |\eta|L_2 + c|\psi|L_3) / (\xi^2 + \eta^2 + c^2\psi^2)^{1/2}, \quad (25.17)$$

where ξ is longitudinal creep; η is lateral creep;

$$c = \sqrt{ab};$$

coefficients L_1, L_2, L_3 are defined with the help of the approximate expressions:

for $b < a$

$$L_1 G / a = -0.119 - 0.486\beta + 1.25\sqrt{\beta};$$

$$L_2 G / a = -0.142 - 0.337\beta + 1.207\sqrt{\beta};$$

$$L_3 G / a = -0.122 - 0.383\beta + 1.039\sqrt{\beta};$$

for $b > a$

$$L_1 G / a = 0.818 - 0.196\beta + 0.024\sqrt{\beta};$$

$$L_2 G / a = 1.112 - 0.519\beta + 0.133\beta^2 ;$$

$$L_3 / a = 0.527 + 0.428\beta - 0.719\beta^2 + 0.298\beta^3 .$$

The angular velocity of wheelset rotation is equal to $\omega = V / r_k$, where V is railway vehicle speed, r_k is rolling radius of the wheel.

The wheel profile is assigned deterministically by using the coordinates of points. The contact patch is divided into longitudinal strips oriented along the rolling direction chosen by the lines passing through the given points as previously. The distribution of the tangential stresses is defined sequentially for every strip.

Let us consider the strip i chosen by the lines passing through the two adjoining points (figure 25.11). Its half length x_{i1} was defined at the solution of the normal contact problem. The strip is divided into surface sections with size Δs along the rail profile and prescribed size Δz along the strip length. The definition of the tangential stresses for every section j is carried out sequentially beginning from the section adjacent to the front edge B . Pressure on front edge B is supposed to be zero therefore the components of the tangential stresses are also equal to zero: q_z oriented along axis z passing in the rolling direction; q_s tangential to the rail profile.

For the definition of the tangential stresses on the contact surface, algorithm FASTSIM uses the rigid slips. Rigid slips represent the relative slip velocity (creeps and spin) of the point j of a wheel relatively the corresponding point of a rail on the assumption that the contacting bodies are absolutely rigid. One of components of the rigid slip along the rolling direction is equal to the longitudinal creep ξ for all points. One of component of the rigid slip in the lateral direction tangential to the rail profile equals to $\eta_s = \eta / \sin \alpha_i$ (figure 25.12e).

The rigid slips are defined based on assumption that the wheelset as a rigid body rolls on rigid rails. Instantaneous axis passes through the points of initial contact 1 and 2 (figure 25.12d). The difference of the radii of rolling of wheels Δr is small in comparison with the distance S between wheels rolling circles therefore it may be assumed that angle θ between instantaneous axis and wheelset axis is small and vector ϖ is parallel to wheelset axis. In case of the multipoint contact, such point is situated on rolling surface of the rail. In this case, the normal force on the rolling surface is usually larger than in the flange contact. Friction coefficient in the rolling surface contact is also larger as a result of the application of lubricators decreasing constant of friction in the flange contact. Therefore it may be assumed that there is no sliding in point of initial contact on the rolling surface. In case of conformal contact, instantaneous axis passes through the points C that is the point of resultant force application.

Velocity of the point j of flange at rotation round instantaneous axis is equal to

$$v_j = \omega \rho = \frac{V}{r_k} \rho ,$$

where $\rho = \sqrt{y_j^2 + z_j^2}$, coordinates y_j, z_j are counted from the instantaneous axis of rotation (figure 25.12f).

Its z component gives the component of rigid sliding along z axis

$$\frac{1}{V} v_j \cos \varphi = \frac{1}{V} \frac{V}{r_k} \rho \frac{y_j}{\rho} = \frac{y_j}{r_k},$$

and rigid sliding of the point j along z axis is equal to

$$w_z = \xi + \frac{y_j}{r_k}.$$

Projection of component $v_j \sin \varphi$ on tangent to the wheel profile in the point j gives component of lateral rigid sliding

$$\frac{1}{V} v_j \sin \varphi \cos \alpha_i = \frac{1}{V} \frac{V}{r_k} \rho \frac{z_j}{\rho} \cos \alpha_i = \frac{z_j}{r_k} \cos \alpha_i,$$

and lateral rigid sliding is equal

$$w_s = \frac{\eta}{\sin \alpha_i} + \frac{z_j}{r_k} \cos \alpha_i.$$

Components of the tangent stresses parallel to the axis z and tangential to the rail profile are determined by the equations

$$q_{zj} = q_{z,(j-1)} + w_z \Delta z / L, \quad (25.18)$$

$$q_{sj} = q_{s,(j-1)} + w_s \Delta z / L, \quad (25.19)$$

where $q_{z,(j-1)}, q_{s,(j-1)}$ are components of the tangent stresses on the surface section j-1.

Values of the longitudinal and lateral creep forces for a strip are determined as a sum of the resultant stresses on its sections

$$F_x = \sum_{k=0}^{n_j} q_{sk} \Delta s \Delta z \sin \alpha_k; \quad (25.20)$$

$$F_z = \sum_{k=0}^{n_j} q_{zk} \Delta s \Delta z, \quad (25.21)$$

where n_j is the number of segments of the considered strip.

The creep forces appeared in the contact of wheel and rail are obtained by summation of the forces on all strips.

The contact problem for a railway wheel with the DMETI profile and the rail R65 with new surface is considered as a test problem. The solution is obtained by means of the finite element method by using model containing 321510 nodes. The distribution of the contact pressure at value of the normal contact force of 139 kN is shown in figure 25.13a. The same problem was solved with the help of the fast algorithm at the prescribed parameters: penetration $\delta = 0.131$ mm, penetration factor $K_B = 0.53$, pressure factor $k_p = 0.35$. The normal contact force obtained at the prescribed penetration is 127 kN. Error of its definition is equal to 8.6 %. The distribution of the contact pressure in section $z = 0$ obtained by using the fast algorithm is shown in figure 25.13b.

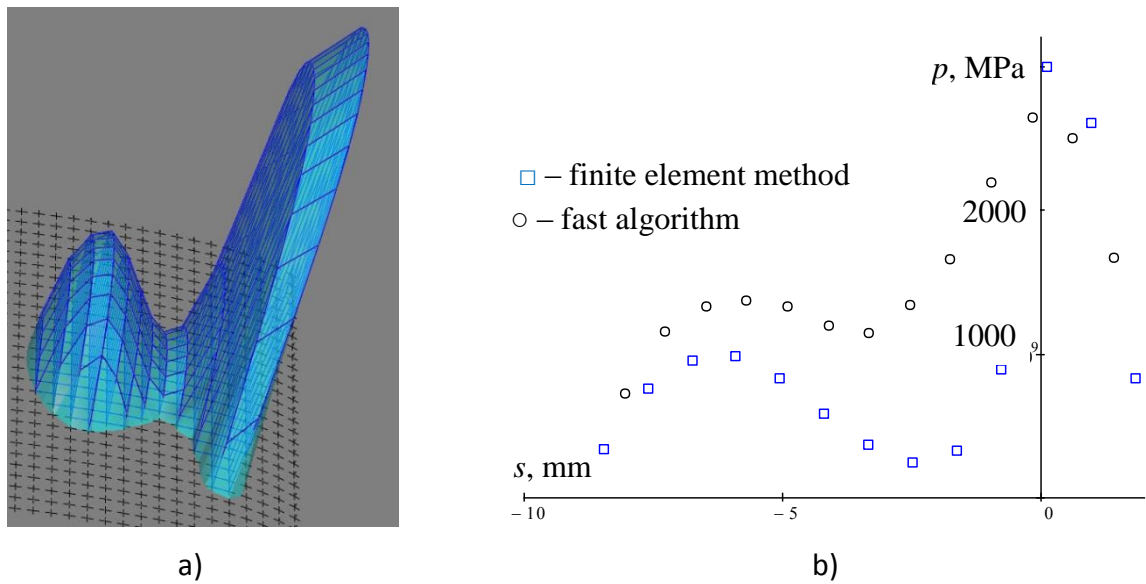


Figure 25.13. Distribution of contact pressure in contact of the wheel with profile DMeTI and the rail R65 obtained using: a – finite element method; b – fast algorithm

For the car wheel with tread wear of 1 mm and the new rail R65, the multipoint contact is occurred for one of relative positions (figure 25.9b). The distribution of the tangential forces is shown in figure 25.14b at the following values of parameters: resultant normal force $N = 90$ kN, longitudinal creep $\xi = -0.00075$, lateral creep $\eta = 0.00017$ and spin $\psi = -0.2115$.

The conformal contact has place for the wheel with linear wear of the tread of 1 mm and the rail R65 with side wear of 5.5 mm (figure 25.9a). The distribution of the tangential forces is shown in figure 25.14a at the following parameters: normal force $N = 160$ kN, longitudinal creep $\xi = -0.00045$, lateral creep $\eta = 0.00036$ and spin $\psi = -0.9257$.

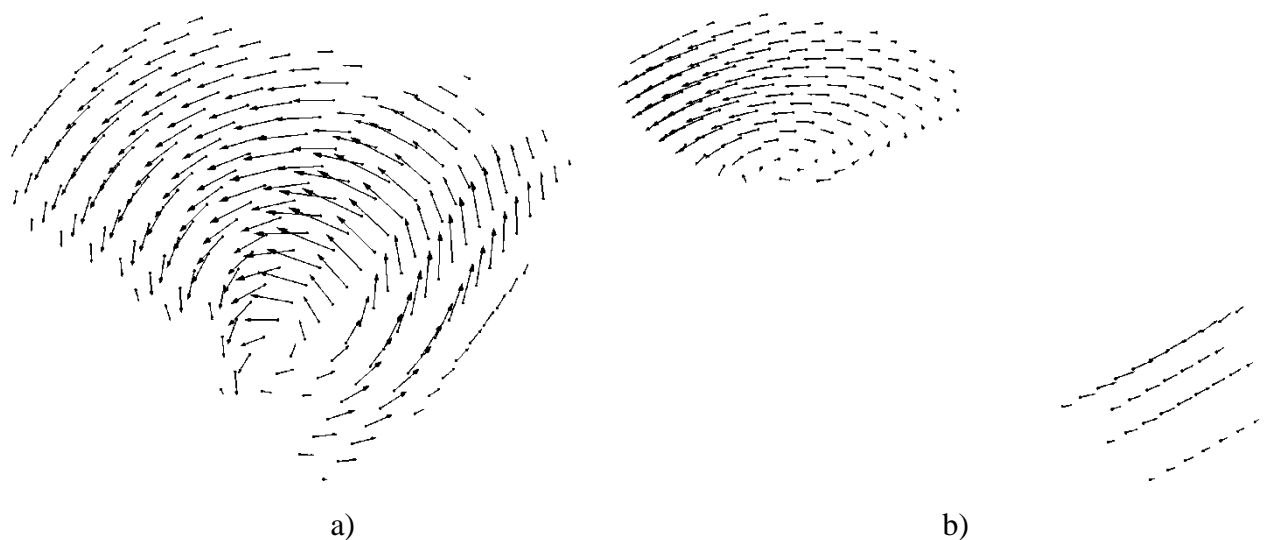


Figure 25.14. Distribution of the tangential forces on the surface of contact: a – conformal; b – multipoint

25.4. Modeling accumulation of contact fatigue damage in UM RCF module

25.4.1. Input data

For simulation of accumulation of contact fatigue damages in **UM RCF** module it is required two types of input data:

- information about the wheel and the rail profiles;
- simulation results of dynamics of wheel on rail.

Initial data about wheel and rail profiles includes the follows:

- wheel radius;
- coordinates x and y of wheel profile points;
- coordinates x and y of rail profile points;
- weight coefficient of *alternative* in the families of *alternatives* (User's manual, [Chapter 16](#), Sect. 16.1).

The coordinates of profile points are assigned with step 0.1 mm along the profile line. Profile points are assigned from the left to the right in the same coordinate system Oxy , wheel flange should be at the right side. The point of the wheel profile placed on the rolling circle must be common origin of coordinates for the wheel and the rail profiles. The maximum stress in any radial section of the wheel appears once for one revolution of the wheel since rolling generates periodical loading. Hence, in **UM RCF** module the accumulated fatigue damages are assigned to one radial section of the wheel.

UM Loco handles one- or two-point contact (User's manual, [Chapter 8](#), Sect. 4). Therefore, the information about two contact points is transmitted to the **UM RCF** module as input data. Data for calculation in module **UM RCF** is prepared in the form of array which dimension is equal to the number of revolutions of the wheel on a prescribed distance. Each element of this array named hereinafter *run step* contains following information.

- Angle of rotation of the wheel relatively longitudinal axis of the rail.
- Friction coefficient for the first point of contact.
- Index of wheel tread contact point of the wheel profile.
- Index of rail contact point of the rail profile.
- Value of normal force N_1 in the first contact point.
- Longitudinal creep in the first contact point.
- Lateral creep in the first contact point.
- Spin in the first contact point.
- Friction coefficient for the second point of contact.
- Index of wheel flange contact point.
- Index of rail contact point.
- Value of normal force N_2 in the second contact point.
- Longitudinal creep in the second contact point.
- Lateral creep in the second contact point.
- Spin in the second contact point.

Besides data that necessary for execution of calculation listed above, files of source data contain subsidiary information: time and rate of movement, radius of curvature of rail track, wear of wheel on previous iterations, kilometrage, reduction coefficients and others.

25.4.2. Creation of finite element mesh of the wheel

Dimensions of used meshes for solution of wheel/rail contact problems are chosen so as to provide minimum computer time and sufficient accuracy of results. The wheel and rail profiles are assigned with coordinates of the points placed with step 0.1 mm. Preliminarily analysis showed that reasonable balance between complexity of the FE-mesh and accuracy of solution is provided by finite elements with dimensions about 1 mm. FE-mesh of wheel fragment contains 7-10 layers of finite elements adjacent to contact surface.

Creation of finite element mesh starts with building of flat mesh of quadrangular finite elements. It is built on the base of nodes placed on the wheel profile with 1 mm step (figure 25.15). Dimension of the scheme along the wheel profile is equal to 105 mm. It covers the profile section where contact has place at any possible locations wheel on rail. Then it is built three-dimensional mesh. Flat mesh is dragged along circular arc by revolution around an axis of the wheelset (figure 25.16). Dimension of mesh at circular direction is amount to 50 mm. This dimension is chosen with taking into consideration that contact patch length does not exceed 50 mm in any case.

The thickness of fragment of 10 mm ensures sufficient accuracy of solution by using elastic foundation. The most probable dimension of semiaxis a of contact patch does not exceed 10 mm and point with the most tangential stress is placed on depth about $0.5a$. However such a small wheel fragment includes zone with the most stresses. Nevertheless the obtained scheme has many degrees of freedom. For example the scheme presented in figure 25.16 contains 59466 nodes and has 178398 degrees of freedom. Therefore in order to decrease simulation time, a fragment of this scheme will be used in calculations (Sect. 25.3.2).

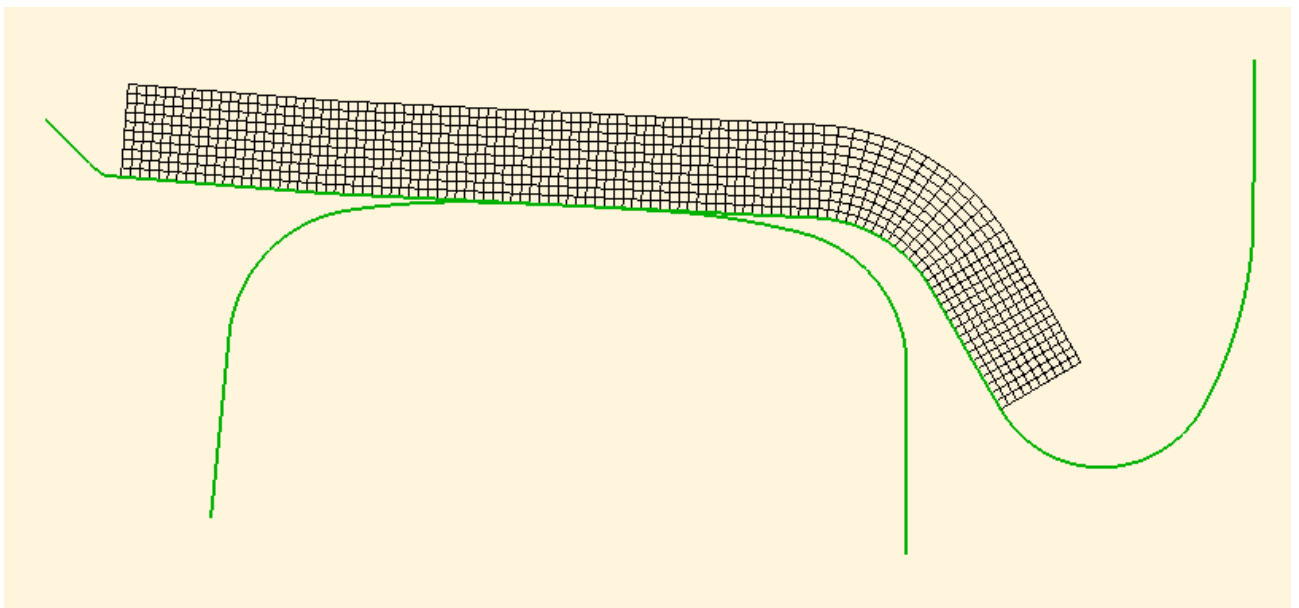


Figure 25.15. Plain mesh for building of FE model of wheel fragment

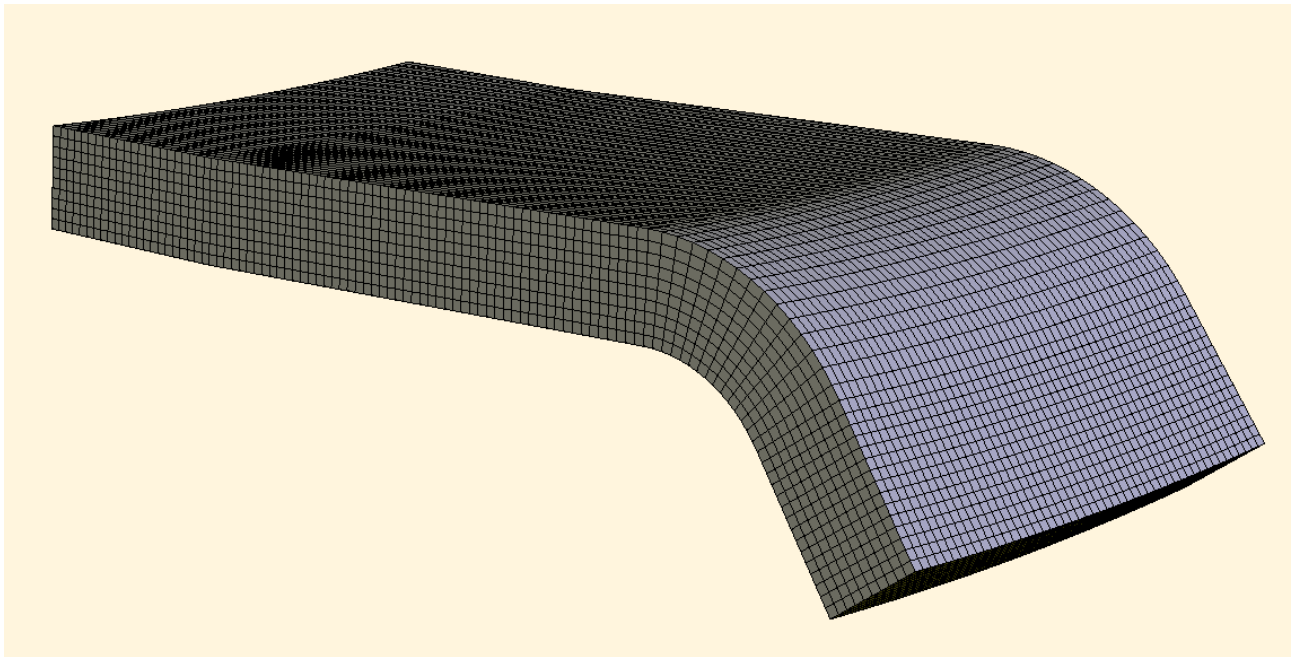


Figure 25.16. Three-dimensional FE model of wheel fragment

25.4.3. Definition of contact forces by using fast algorithm

The contact forces are defined by using the fast algorithm described in Sect. 25.3.3.

Wheel and rail profiles described by points with step 0.1 mm are used for solution of normal contact problem. The form and dimensions of contact patch and contact pressure distribution are defined in the following way.

From initial data on *run step* the following values are taken: normal force N , indices of initial points of contact situated on wheel and rail profiles; angle φ of rotation of the wheel relatively longitudinal axes of the rail. The rail profile is shifted in the lateral direction to the touch of the points of initial contact of wheel and rail and turned on the angle φ .

Then the penetration δ of wheel profile into rail profile, which provides obtaining necessary normal force N value defining by using equations (25.15), is determined (Sect. 25.3.3.2).

In [22] it was established that dependence between force and penetration is close to linear in the range of forces 50...150 kN. Taking into account this fact it is enough three iterations to calculate the penetration δ . The value of normal force is defined for preset penetration values of 0.05 and 0.1 mm. It gives us a possibility to determine the linear dependence between force and penetration as

$$\delta = kN + b$$

With applying of this dependence, the necessary penetration δ corresponding to the known value of the force N is defined. Penetration coefficient K_B is accepted 0.53, coefficient k_p is defined by using equation (25.10) (Sect. 25.3.3.1).

For determination of form and dimensions of contact patch the penetration $\delta_0 = K_B \delta$ is used. Coordinates of the points situated on front edge of the contact are defined with applying of the dependence (25.12) (Sect. 25.3.3.2).

Normal forces in nodes of finite element mesh are defined as

$$N_i = p_i \Delta s \Delta z,$$

on the assumption that pressure p_i is distributed in accord with the elliptical law and is defined using dependence (25.13), Sect. 25.3.3.2.

Tangential forces in nodes of finite element mesh are defined using dependences (25.20) and (25.21), Sect. 25.3.3.3.

In case of double-point contact (Sect. 25.4.1), the above procedure of selection of the penetration is performed separately for each contact.

25.4.4. Definition of stresses in area of wheel and rail contact

In the section above the definition of form and dimensions of contact patch and values of forces in nodes are obtained. After that a small fragment (figure 25.17a) is separated from initial finite element mesh (Sect. 25.4.2). Dimensions of the mesh bordering upon contact surface are assigned so that it exceed dimensions of contact patch at every direction on 3 mm. It has thickness of the same dimension.

The application of the finite element fragment on elastic foundation as a design scheme allows to define stress and strain in 3D region bordering to contact surface without any type of simplified assumptions like a contact patch has form of circle or ellipse or a contact patch is plane. Using such fragment allows to decrease computer time essentially (par. 25.3.2).

The components of stiffness matrix of that small fragment are calculated on the creation of FE-mesh. Spring constrains are put on nodes situated on all surfaces of small fragment except contact surface, (figure 25.17b). The stiffness of constrains is accepted to be 10^7 N/m according to recommendations from [22].

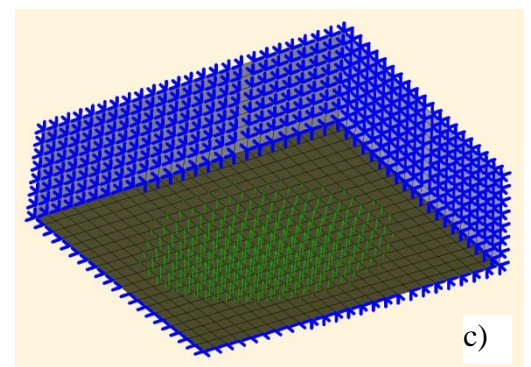
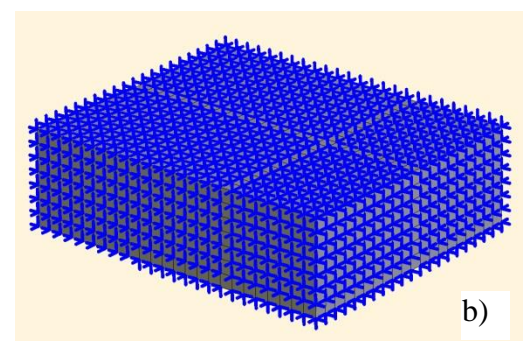
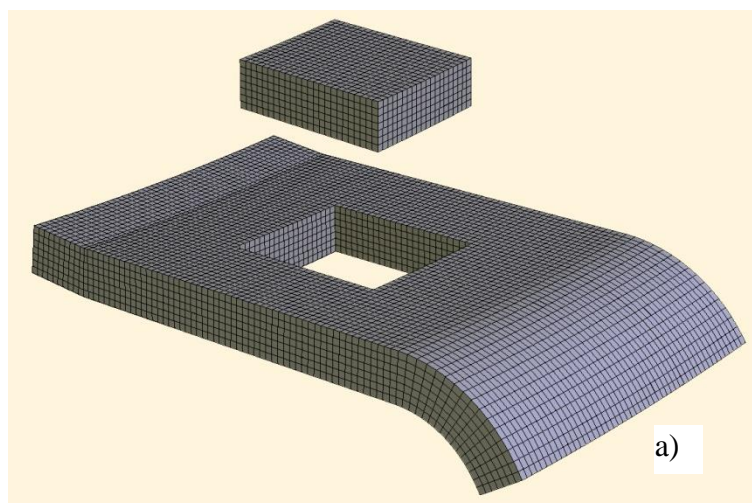


Figure 25.17. Finite element fragment on elastic foundation: a) separation of small fragment from initial finite element scheme; b) applying of elastic constrains on surfaces of separated fragment; c) applying of forces to nodes of contact surface of separated fragment.

Components of the stiffness matrix of finite element ensemble adjacent to an internal node of the fragment are taken from the stiffness matrix built for the initial calculation scheme. For nodes situated on the fragment surface, the components are halved, for nodes situated on edges are divided into four.

The contact forces are applied to nodes on the contact surface of the separated fragment (figure 25.17c). Displacements of the nodes are defined with the method of node iterations [17]. This method ensures two advantages: the algorithm assigned for the solution of contact problems is used; number of iterations may be limited when the sufficient accuracy of solution is obtained. Twenty five iterations are normally enough.

Stresses are calculated for nodes of finite elements bordering upon lateral plane of symmetry of the contact area from every side. Using its values for nodes situated in plane of symmetry, Dang Van's reduced stresses τ_{DV} are calculated. At modeling of fatigue damages accumulation process, Dang Van's reduced stresses are compared with damaging stresses. The areas of equal stresses τ_{DV} in coloring and isolines of these stresses are shown in figure 25.18. The example of calculation is presented below. The greatest stress $\tau_{DV} = 122$ MPa is obtained for the node situated in depth of 4 mm under contact surface.

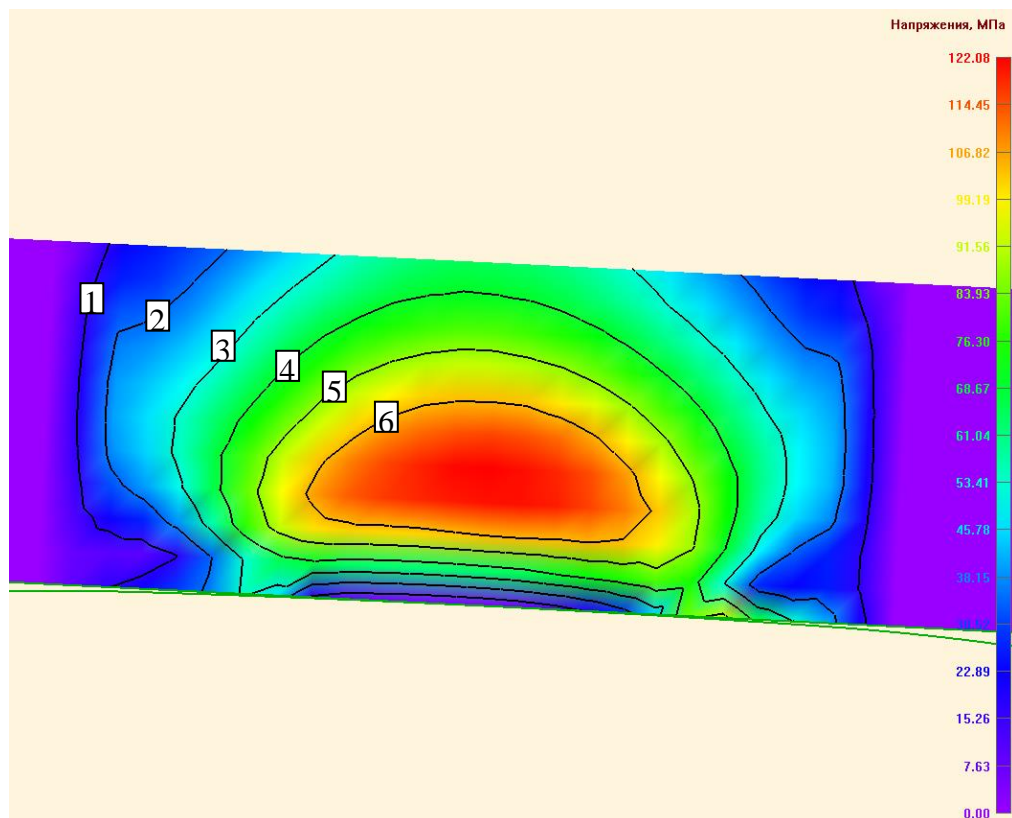


Figure 25.18. Areas of equal τ_{DV} in lateral section of the wheel passing along symmetry plane of contact; 1-6 – numbers of lines of equal τ_{DV} , value of isoline 17,44 MPa

25.4.5. Damages accumulation in nodes of finite element mesh

Number of cycles until fracture for nodes situated in plane of symmetry is calculated with the help of equation (25.4). Accumulated damage in a point of wheel is defined by summing of damages (Sect. 25.2.4)

$$Q(x, y, z, t) = \sum \frac{1}{N(\tau_{DV})}, \quad (25.22)$$

where $N(\tau_{DV})$ is number of cycles until fracture of material under level τ_{DV} of reduced stress.

In circular contact at maximum pressure $p_0 = 1000$ MPa, the point with the greatest tangential stress τ_{\max} equal to $0.32p_0$ situates on the axis z directed from the center of contact patch in depth of $0.5a$, where a is the radius of the contact patch. Normal stress in this point is calculated as follows:

$$\sigma_x = \sigma_y = -0,18p_0, \quad \sigma_z = -0,8p_0.$$

Then for this point it is obtained

$$\tau_{DV} = \tau_{\max}^a + a_{DV}\sigma_0 = \frac{1}{2}0,32p_0 - 0,1 \cdot 0,387p_0 = 0,12p_0 = 120 \text{ MPa.}$$

Cycle is considered as damaging one if stress τ_{DV} exceeded 120 MPa at modeling of accumulation of contact fatigue damages. Thus working section of the contact fatigue curve obtained by means of extrapolation is from $8 \cdot 10^5$ to $16 \cdot 10^5$ cycles (Sect. 25.2.3). However, the desired minimum damaging stress, which is equal to 120 MPa, can be changed by the user (Sect. 25.5.4.2).

25.4.6. Consideration of wear of the wheel profile

Procedure of accumulation of contact fatigue damages in nodes of finite element scheme of wheel described above is executed along with *wear iteration*, at which wheel profile is not changed (User's manual, [Chapter 16](#), Sect. 16.1). Many iterations can be considered in the case of using of wheel wear evolution procedure provided by **UM Wheel\Rail Wear**. After execution of *wear iteration* in the **UM Wheel\Rail Wear** module, the wear diagrams is defined and wheel wear for each node is calculated by changing the coordinates of the nodes that lie on the surface of the contact.

Thus the **UM RCF** module gets new initial data and the changed wheel profile. The coordinates of all nodes of profile are recalculated. Nodes are moved along the normal to the contact surface on the amount of wear. The initial FE-mesh is reconstructed. Now it is built on the basis of a worn wheel profile. Damages assigned to the nodes of new mesh are calculated by interpolation accumulated damages in nodes of previous mesh. Next, the procedure of accumulation of contact fatigue damages in the nodes of the new FE model of wheel is repeated.

25.5. Working with UM RCF module

25.5.1. Running UM RCF module

The **On** check box must be checked on the **Evolution | Rolling contact fatigue** tab of scanning project window to perform the calculation by using the **UM RCF** module (figure 25.19). The wheels, for which the calculation will be performed, should be checked at the same tab. In this case input data files and ***.rcf** project file for the calculation of rolling contact fatigue will be created after the finish scanning project. To run the module click **Run** button at the **Results | Railway profiles** tab (figure 25.20). The correspondent ***.rcf** project, created as a result of the scanning project, will be loaded. The **Run** button is not active, if the scanning of the project was not carried out.

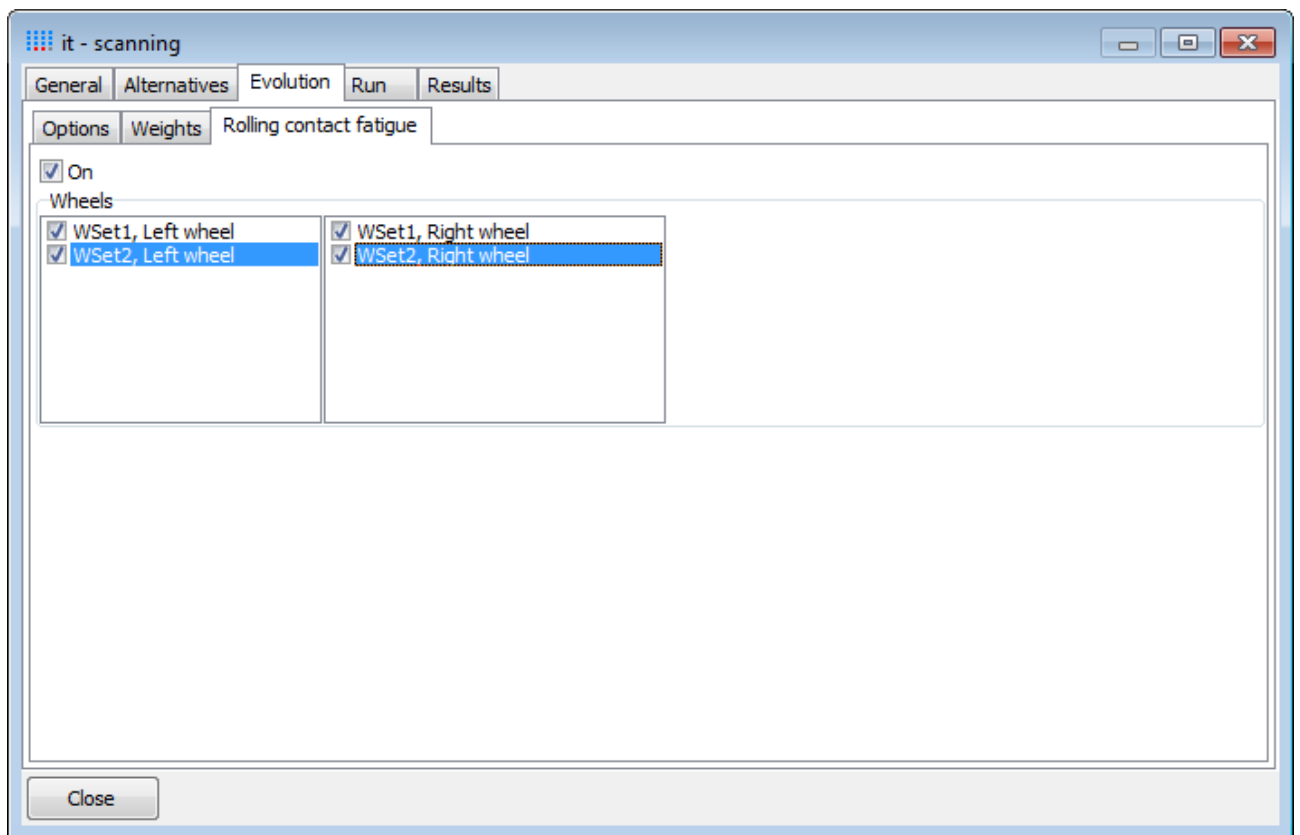


Figure 25.19. Rolling contact fatigue in UM Simulation

UM RCF module can be run autonomously by using **Start | All Programs | Universal Mechanism 7 | Tools | Rolling Contact Fatigue** menu. In this case user has to load a project file ***.rcf** by using the **File | Open** menu or a button  on the **Standard** toolbar.

The ***.rcf** project file is a text file. It prescribes the file paths with the input data of the two types (Sect. 25.4.1).

The **dpf**-files include information about wheel and rail profiles. DPF-files are of a text format.

The **dnm**-files include simulation results of modeling the dynamics of wheel at the rail. Files of this type are of a binary format.

The **rcf**-file contains the names of *alternatives* and values of kilometrage on each *wear iteration*.

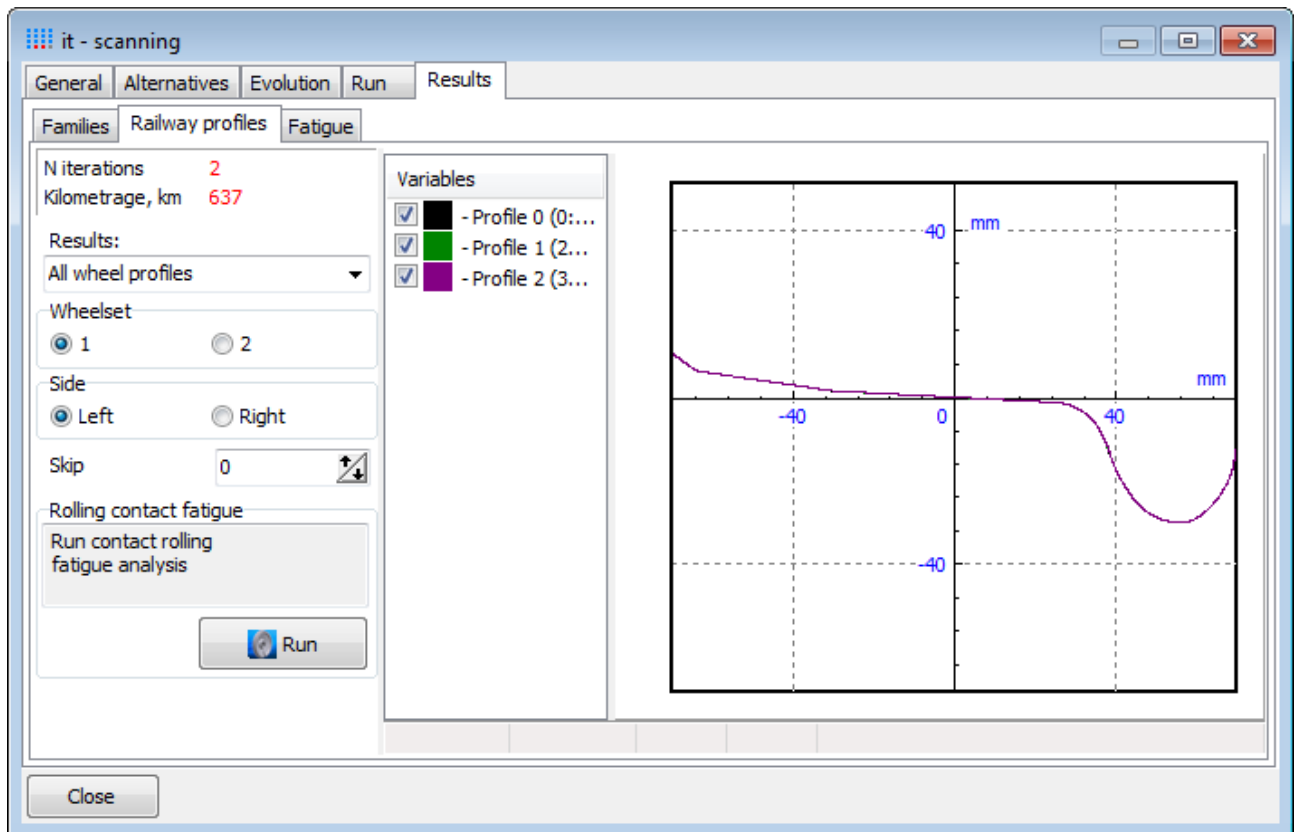


Figure 25.20. Starting the **UM RCF** module from the **UM Simulation**

25.5.2. Interface of the module

Interface of the **UM RCF** module is presented in figure 25.21.

In the top of the window the title bar, menu bar, **Standard** toolbar and **Design Scheme** toolbar are located. In the bottom the status bar is located. In the left side of the window the floating **Information Panel** is placed. The user can dock it to the left or right side of the window or hide it. By default, the **Information Panel** is attached to the left side of the window and is always visible whenever you start the module.

The user can show or hide the toolbars and **Information Panel** and change its settings by the **View | Toolbars and Docking Windows** menu or using the context menu by clicking the right mouse button. The user can also change the appearance of the module window using the **View | Application Look** menu.

The workspace window is intended for graphical displaying of design scheme and results of calculations. If the data to calculate was loaded, in the center of the work area always is displayed the wheel and rail profiles by green lines. Those lines cannot be hidden; all other display modes can be switched on or off, for example, using the buttons on the **Design Scheme** toolbar. During calculations the **Coloring mode** is activated automatically. Equivalent stresses in the median plane of the finite element fragment are shown in the bottom. The cumulative fatigue damages in the same plane are shown on top. The color scale for assessing the level of accumu-

lated damages is on the left and the color scale for the assessment of equivalent stress is on the right.



Figure 25.21. Interface of the **UM RCF** module

Creation of finite element fragment of the wheel is considered in details in Sect. 25.4.2, calculation of equivalent stresses is considered in Sect. 25.4.4, accumulation of contact fatigue damages is presented in Sect. 25.4.5.

25.5.3. Overview of the buttons on the "Design Scheme" toolbar

The **Design Scheme** toolbar, which is located by default at the top of the window, is shown in figure 25.22. Below the brief description of each button on the panel is presented. Note that the same options are duplicated in the **Design Scheme** menu and have the keyboard shortcuts.



Figure 25.22. Design Scheme toolbar

 – Run (F9)

-  – Stop (Esc)
-  – Previous alternative (PgDn)
-  – Next alternative (PgUp)
-  – Delete results of calculation (Del)
-  – Delete stiffness matrix (Ctrl+Del)
-  – Mesh (1)
-  – Coloring (2)
-  – Isolines (3)
-  – Maximum damage (4)
-  – Numbers of nodes (5)
-  – Starting position (Home)
-  – Parameters

The detailed description of each of these options is below.

25.5.4. Parameters

The "Parameters" option becomes active when the data for calculation is loaded. After selecting it by using the **Design Scheme | Parameters...** menu or by the button  on the screen the dialog box will be displayed, which is shown in figure 25.23.

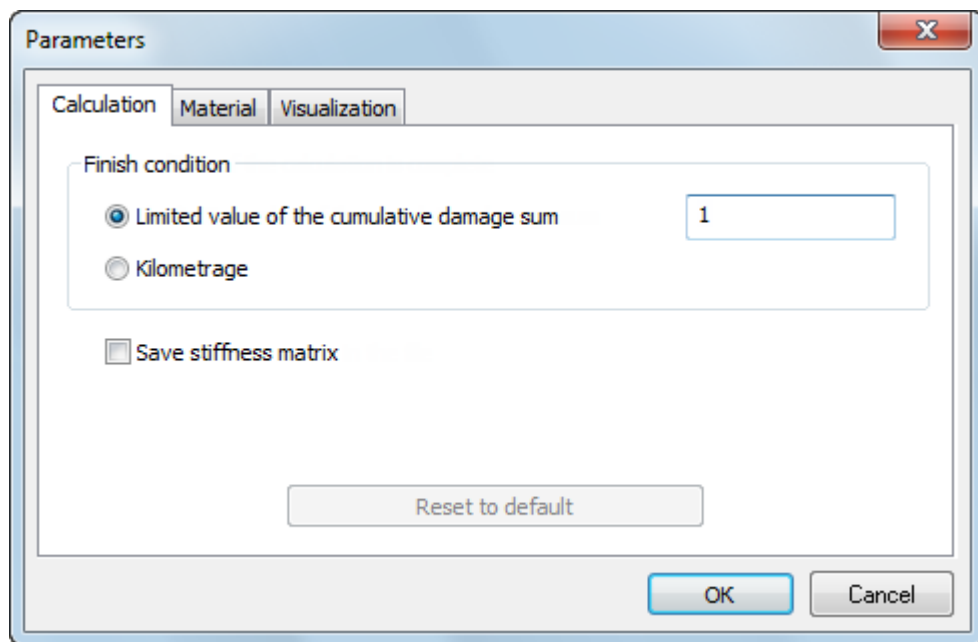


Figure 25.23. The "Parameters" dialog box, the **Calculation** tab

The dialog box has three tabs: **Calculation**, **Material** and **Visualization**. The **Reset to default** button allows back to the original values of the parameters at the selected tab. Saving the changed parameters occurs only after clicking **OK**. Otherwise, the changes will not be saved.

25.5.4.1. The «Calculation» tab

The **Calculation** tab is shown in figure 25.23.

Modeling the accumulation of contact fatigue damages in the **UM RCF** module provides two variants of the finish condition:

- 1) the reaching of limit of cumulative damage sum in the wheel;
- 2) the running of whole distance specified at the modeling of dynamics of the railway vehicle (kilometrage).

In the first case the user has to set the limit value of cumulative damage sum. The accumulation of damages at the point of wheel is calculated by using the dependence (25.22), the accumulation of damages in the nodes of finite element scheme is reviewed in Sect. 25.4.5.

In the second case the calculation will be performed for all the files listed in the ***.rcf** project, regardless of the accumulated damages in the wheel.

By default, the first variant is chosen (**Limited value of the cumulative damage sum**) and **1** is set.

The calculation of each new *wear iteration* begins with the preparing the stiffness matrix of finite element fragment of the wheel (par. 25.4.2, par. 25.4.6). This operation can take several minutes, depending on your computer. In this connection, the total expenditures of the computer time significantly increases, particularly if the calculation is performed for tens or hundreds of *wear iterations*. In any case, it fails to avoid these expenditures at the first. But this possibility appears if necessary to repeat the calculation for the same scheme with other conditions.

The checked option **Save stiffness matrix** means that the stiffness matrix for each new wear iteration will be saved in the ***.smx** file. This file has a binary format and is located in the same folder as the file with the initial data, its size is greater than 100 MB. So you need to have enough free space in the partition of the hard drive where the files are stored. Now, during the calculation the components of the stiffness matrix will be loaded from a file but not calculated, that minimizes the computer time.

However, use of this option carefully. Stiffness matrix depends on the number of nodes of the finite element mesh; the coordinates of nodes of the finite element mesh; Young's modulus E and Poisson's ratio μ .

If the coordinates of points of the profile, the dimensions of finite element scheme, the Young's modulus or Poisson's ratio were changed before the repeated calculation, the stiffness matrix must be formed anew. Accordingly, the old matrix must be destroyed. The algorithm incorporated in the **UM RCF** module works as follows: first, an attempt is made to open a ***.smx** file corresponding to the initial data files (matching is done by file name). If such a file exists, the components of the matrix are loaded from file, if not, the components of the stiffness matrix are calculated.

Note. If initial data was changed then is necessary delete the old stiffness matrices before starting the new calculation. Otherwise it will lead either to incorrect results.

The module reacts on changes material parameters, but cannot react on all the possible actions of the user. For example, if changes to the files of initial data are made outside of the module **UM RCF** or software package **UM**. For this reason, the **Save stiffness matrix** option is inactive by default.

If there is no need to save CPU time, and there is no assurance that the files of old stiffness matrices does not exist, before recalculation it is recommended to remove the files of old stiffness matrices. This can be done by the **Design Scheme | Delete stiffness matrix** menu or by  button.

The **Save stiffness matrix** option can be useful in two cases.

1. The calculation has been interrupted, the module is closed. After restarting the module and resuming the calculation is necessary to form the stiffness matrix for current *wear iteration*. If before that it was saved in the file, then the components of the matrix will be quickly loaded from the file.
2. The calculation was carried out with the specific conditions at the **Calculation** tab. For example, the finish condition of calculation – the limited value of the cumulative damage sum is equal 1. User decides to repeat the same calculation by changing the limit value of accumulated damages or by selecting **Kilometrage** option. In this case, you must delete the result files and return to the beginning of the calculation. The files of stiffness matrix will be deleted and recalculation will run much faster.

If was changed the condition of ending calculation at the **Calculation** tab, then after clicking the **OK** button, a dialog box appears, see figure 25.24.

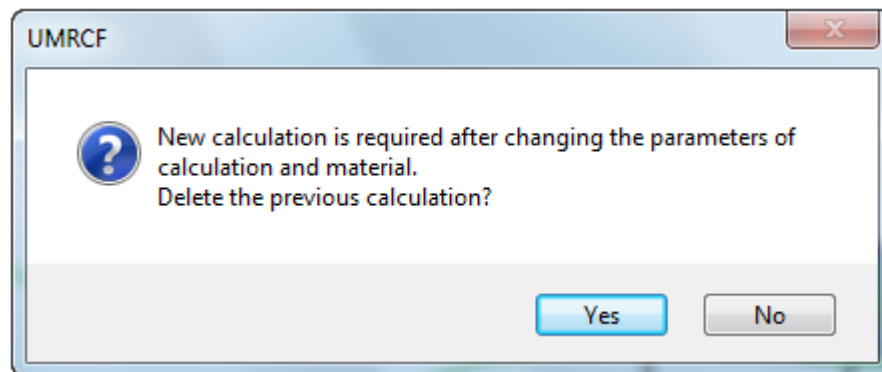


Figure 25.24. Request to remove the results of the calculation

The **No** button means parameter changes will not be saved.

The **Yes** button means that parameter will be saved and files with the simulation results will be deleted. The stiffness matrix files, if they had previously been created, will not be deleted. After that one can run the calculation with the new parameters.

25.5.4.2. The «Material» tab

The **Material** tab is shown in figure 25.25.

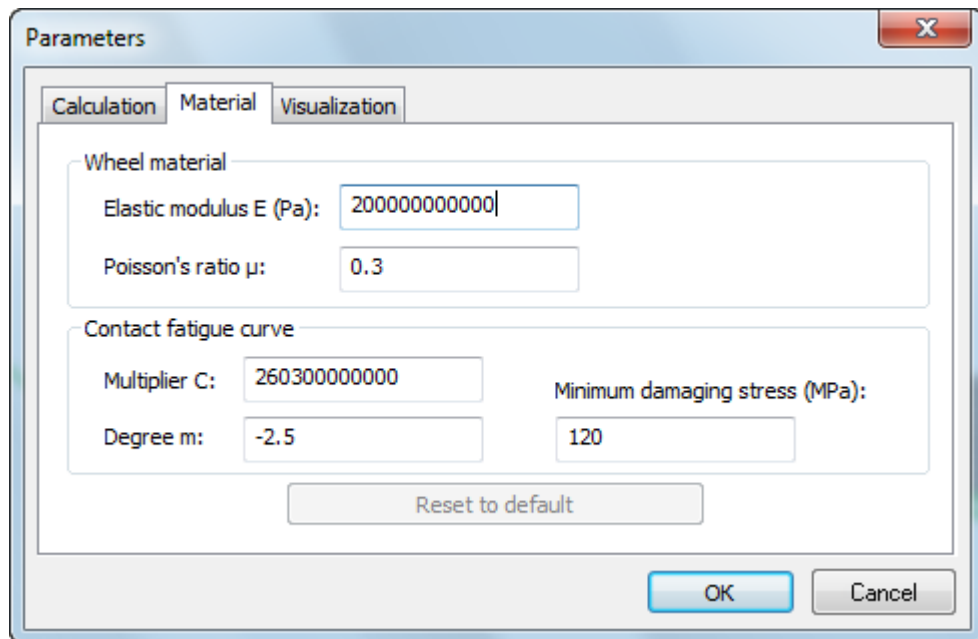


Figure 25.25. The "Parameters" dialog box, the Material tab

Young's modulus E ($2 \cdot 10^{11}$ Pa by default) and Poisson's ratio μ (0.3 by default) can be assigned at the tab. The contact fatigue curve is approximated by the function of the following form (Sect. 25.2.3)

$$N = C \tau_{DV}^m,$$

where N is number of cycles until fracture;

τ_{DV} is reduced stress based on Dang Van's criterion.

The default values of multiplier $C = 2.603 \cdot 10^{11}$ and degree $m = -2.5$ are obtained for wheel steel (par. 25.2.3). The minimum level of damaging equivalent stress of 120 MPa is proven in Sect. 25.4.5.

If any of the parameters at the **Material** tab was changed, then after clicking the **OK** button, a dialog box appears as shown in figure 25.24.

The **No** button means exit without saving changed parameters.

The **Yes** button means exit with saving changed parameters. The result files and the stiffness matrix files will be deleted. After that one can run the calculation with the new parameters.

25.5.4.3. The «Visualization» tab

The **Visualization** tab is shown in figure 25.26.

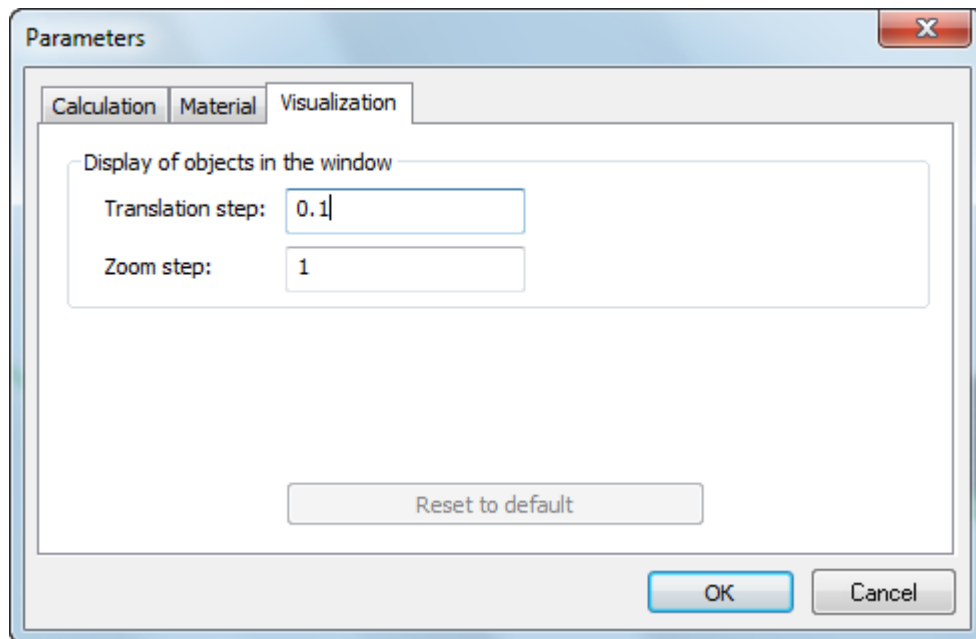


Figure 25.26. The "Parameters" dialog box, the **Visualization** tab

The design scheme can be moved in the window in any direction by using the arrow keys on keyboard (or the left mouse button), it can be increased or decreased by pressing the «Gray +» and «Gray -» (or mouse wheel). All these operations are performed discretely with a determined step. User can change the step values at the **Visualization** tab. The steps are assigned in conventional units.

By default **Translation step** is 0.1, **Zoom step** is 1.

25.5.5. Imaging modes

As described above, if the data for the calculation is loaded, the wheel and rail profiles are shown in the window. Besides that, the module supports imaging modes of the design scheme and of the calculation results: **Mesh**, **Coloring**, **Isolines**, **Maximum damage**, **Numbers of the nodes**. Modes can be turned on or off in various combinations with each other.

If necessary, the design scheme in the window can be moved, zoom in or out. The scheme can be returned to its original position in the following ways:

- choose the **Design Scheme | Starting position** menu;
- click the button  at the **Design Scheme** toolbar;
- click the **Home** key at the keyboard;
- right-click on the window, the shortcut menu, select the **Starting position**.

25.5.5.1. Mesh

There are three ways enable or disable the **Mesh** imaging mode:

- choose the **Design Scheme | Mesh** menu;
- click the button  at the **Design Scheme** toolbar;
- click the button **1** at the keyboard.

The mesh from quadrangular elements, which is located at the plane of symmetry of the finite element fragment of wheel, is displayed in the center of window (figure 25.15). If enable the **Mesh** mode, when the **Coloring** mode is enabled, then a similar mesh is displayed in the top of window at the median plane of wheel fragment, where is illustrated the process of accumulation of contact fatigue damages.

The mode is automatically activated when the data is loaded.

Note. The Mesh mode is always available, if data for calculation is loaded.

25.5.5.2. Coloring

There are three ways enable or disable the **Coloring** imaging mode:

- choose the **Design Scheme | Coloring** menu;
- click the button  at the **Design Scheme** toolbar;
- click the button **2** at the keyboard.

The coloring median plane of the wheel fragment is shown in the center and top of window (figure 25.21). For each quadrangular element of flat mesh the color filling is performed. The color of the node is chosen depending on the value of the component and accordance with the scale. Then the resulting colors from the four vertices are mixed in the plane of the element by a linear law. As a component for the median plane of the wheel fragment the following two components are used. The equivalent Dang Van's stresses is shown in the center of window and the accumulated contact fatigue damages are shown in the top part of the window.

Note. The **Coloring** mode is available, if data for calculation is loaded and the calculation was run.

25.5.5.3. Isolines

There are three ways enable or disable the **Isolines** imaging mode:

- choose the **Design Scheme | Isolines** menu;
- click the button  at the **Design Scheme** toolbar;
- click the button **3** at the keyboard.

Black lines are lines of equal values of a component – isoparametric lines, is shown in the center and top of window (figure 25.21). The mode supports six isolines. As in the **Coloring**

mode, components are the equivalent Dang Van's stresses and accumulated contact fatigue damages.

Note. The **Isolines** mode is available, if data for calculation is loaded, the calculation was run and the **Coloring** mode is enabled.

25.5.5.4. Maximum damage

There are three ways enable or disable the **Maximum damage** imaging mode:

- choose the **Design Scheme | Maximum damage** menu;
- click the button  at the **Design Scheme** toolbar;
- click the button **4** at the keyboard.

The node, that has the largest cumulative damage sum, is designated by the circle with a thick white border in the top of window at the median plane of the wheel fragment (figure 25.21). The value of maximum damage can be viewed at the **Information Panel** in the **Calculation parameters** field (figure 25.27).

Note. The **Maximum damage** mode is available, if data for calculation were loaded, the calculation was carried out, the largest accumulated damage is greater than zero and the **Coloring** mode is enabled.

25.5.5.5. Numbers of nodes

There are three ways enable or disable the **Numbers of nodes** imaging mode:

- choose the **Design Scheme | Numbers of nodes** menu;
- click the button  at the **Design Scheme** toolbar;
- click the button **5** at the keyboard.

The nodes of finite element mesh are designated by the brown color in the center of window at the median plane of the wheel fragment. The number of each node is displayed next to it. If the **Numbers of nodes** mode and the **Coloring** mode are turned on, then node numbers are also displayed in the top of window at the median plane of the wheel fragment, where the process of accumulation of contact fatigue damages is illustrated.

Note. The **Number of nodes** mode is always available, when data for calculation is loaded.

25.5.6. Performing calculation

The calculation can be run in the following ways:

- choose the **Design Scheme | Run** menu;

- click the button  at the **Design Scheme** toolbar;
- click the button **F9** at the keyboard;
- right-click on the window, the shortcut menu, select the **Run**.

For the **UM RCF** module, the ***.rcf** project is saved during running multivariate calculation in the **UM** (User's manual, [Chapter 6](#)). RCF project file specifies the paths to the ***.dpf** files with the input data, the name of *alternative* for each source file, kilometrage for each *wear iteration*.

The list of files for calculation is formed in the **UM RCF** module in the following sequence. At first all files related to the first wheel are processed, and then to the second wheel, the third and so on, depending of the number of wheels in the initial project of scanning. Thus, the calculation for the first wheel with respect to *wear iterations* is performed completely in the beginning, and then for the second wheel, etc.

If the finish condition of calculation is reaching the limit of cumulative damage sum and this finish condition is actuated before all *wear iterations* for this wheel have been processed, then not processed *wear iterations* are skipped, and the calculation for the next wheel is performed. If the finish condition of calculation is kilometrage, then calculation is performed for all *wear iterations* of the project.

The scheme is automatically set to the starting position and **Coloring** mode is enabled during the calculation (Sect. 25.5.5.2). This mode can be disable only after stopping calculation. The other imaging modes (Sect. 25.5.5) may be enabled or disabled in the course of calculation; however, most of other options are blocked. **Information Panel** (figure 25.27) helps to trace the calculation of the project.

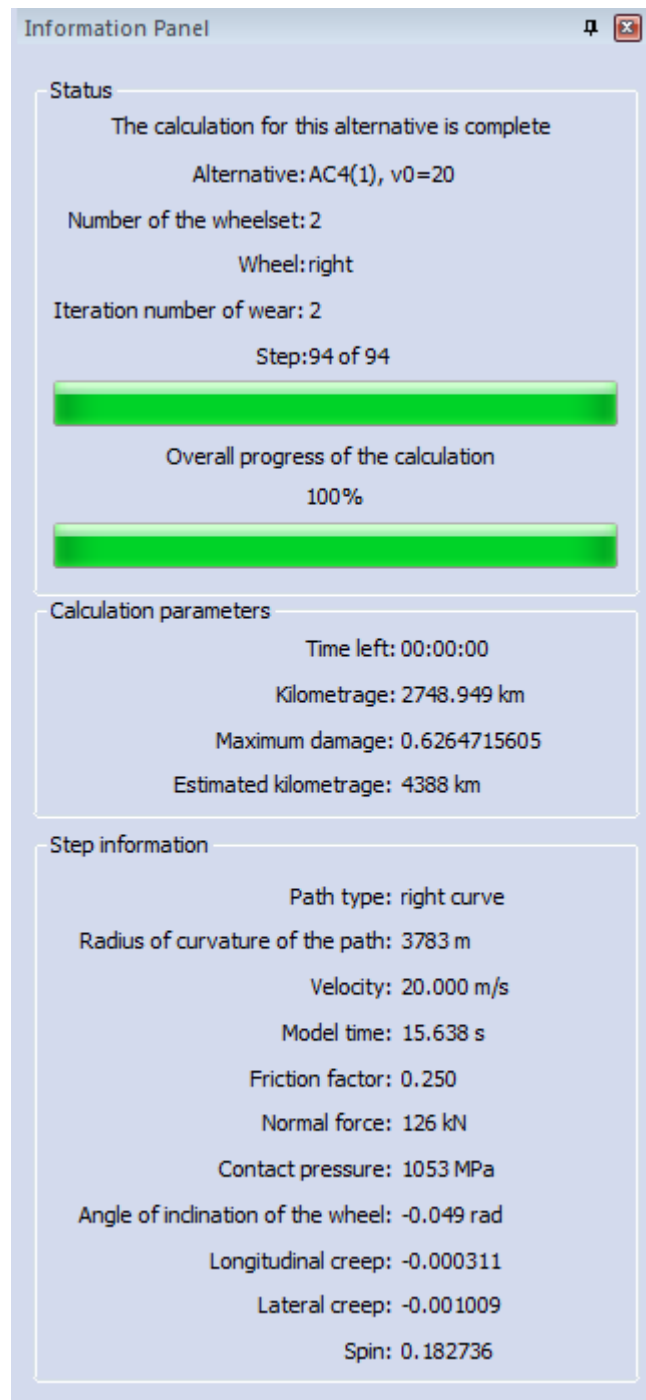


Figure 25.27. **Information Panel**

The wheel is set at the new position relative to the rail at each run step (at each turn). This position is defined by lateral displacement and rotation around the longitudinal axis of the rail. In fact, physically the wheel profile moves relative to the rail. However, in the module, to spend less time for drawing graphic objects in the workspace, the wheel profile together with the finite element mesh remain fixed, and rail profile is moved and rotated. Wheel and rail profiles are shown so as rolling direction of the wheel towards away from the observer. The borders of the contact patches that are defined by using a fast algorithm are displayed by the thick black line in places the contact wheel and rail profiles (Sect. 25.3.3).

The following parameters are displayed at the **Step information** field of the **Information Panel** (figure 25.27): friction factor, the normal force in contact, the pressure, longitudinal and lateral creep, spin, etc. If contact is two-point the details of wheel tread contact are displayed at this field.

The module displays a message in a dialog box on the screen after the calculation is complete.

The calculation can be stopped in the following ways:

- choose the **Design Scheme | Stop** menu;
- click the button  at the **Design Scheme** toolbar;
- click the button **Esc** at the keyboard;
- right-click on the window, the shortcut menu, select the **Stop**.

Note. The **Stop** option is not active, if the calculation is not performed.

25.5.7. Viewing the results of calculation

The **Previous alternative** and **Next alternative** options became available when the calculation is finished. Use **Design Scheme | Previous alternative** and **Design Scheme | Next alternative** menu commands, or by buttons  and  at the **Design Scheme** toolbar, or by keys **PgDn** and **PgUp** at the keyboard to view the results of calculation.

As described in Sect. 25.5.6, all files with input data are arranged in a list formed on the base of numbers of the wheels and *wear iterations*. The **Previous alternative** and **Next alternative** options allow moving through this list from file to file. The calculation results of selected file are displayed at the **Information Panel** and workspace of window.

Help information about the file is displayed at the **Status** field of the **Information Panel**: name of alternative, index of wheelset, wheel – left or right, number of *wear iteration*.

The value of maximum cumulative damage sum and kilometrage are of main interest when the calculation results are analyzed. Both that values are shown at the **Calculation parameters** field of **Information Panel** (figure 25.27). If calculation was carried out to achieve the limit of accumulated contact fatigue damages and this limit has not been reached, the estimated kilometrage shows how many kilometers the wheel could still run at a given level of accumulated damages. The estimated kilometrage is determined by dividing the kilometrage to the greatest cumulative damage sum.

The point of the wheel with the most accumulated damage sum can be marked on the design scheme by using the **Maximum damage** mode (Sect. 25.5.5.4). The depth of this point under the wheel rolling surface may be defined by using the **Mesh** mode (Sect. 25.5.5.1), on the basis that side of the finite element is equal to 1 mm. It is convenient to present the distribution of accumulated contact fatigue damages in a median plane of fragment of the wheel by means the **Coloring** mode (Sect. 25.5.5.2) and **Isolines** mode (Sect. 25.5.5.3).

25.5.8. Saving the results of calculation

The simulation results can be saved by means the **File | Save** menu or a button  on the **Standard** toolbar. This option is disabled during the calculation.

The calculation results are saved in ***.rez** files with the same names as the files with the input data and located in the folder with the original data. The ***.rez** files have text format.

Note. The automatic storage of results after the completion of calculation for each file of input data is supported.

25.5.9. Deleting the results of calculation

The calculation results can be deleted by using the **Design Scheme | Delete results of calculation** menu or a button  on the **Design Scheme** toolbar. The option is available, if the calculation was executed. All folders specified in the ***.rcf** project file will be checked, and all ***.rez** files, found in these folders, will be deleted.

Note. The ***.smx** files with stored components of stiffness matrices will not be deleted!

If necessary to delete the files with stiffness matrix, one can use the **Design Scheme | Delete stiffness matrix** menu command, or a button , or a hot key **Ctrl+Del** (Sect. 25.5.4.1).

Also, all the calculation results, including the ***.rcf** project file, can be removed from the **UM** in the scanning project along with the results of the multivariant calculation.

25.5.10. Samples

UM installation includes two sample projects that are devoted to the simulation of rolling contact fatigue. Sample projects contain a model of two-wheelset railway vehicle. Two variants of speed are given: 15 and 20 m/s. The path of total length of 2750 km is made up of two sections of straight lines and two sections of right curves. The wear of the wheels on the one iteration is taken into account: the railcar movement is continued with the modified profiles of wheels after passing 1488 km. Simulation is performed for the railway vehicle with the two types of wheel profiles: a conical profile of unworn wheel and the curvilinear wheel profile.

These results can be used to demonstrate the operation of the **UM RCF** module.

The path to the files with the input data for a conical profile:

{UM Data}\SAMPLES\Rolling Contact Fatigue\Conical profile of the wheel\it

The path to the files with the input data for a curvilinear profile:

{UM Data}\SAMPLES\Rolling Contact Fatigue\Curvilinear profile of the wheel\it

The **UM RCF** module must be run by any method, referred to in Sect. 25.5.1, to perform a test calculation.

The **data.rcf** project file, placed at the above locations, must be opened, if the **UM RCF** module is running autonomously.

Performing the calculation and analyzing the results are considered in Sect. 25.5.6 and 25.5.7 correspondingly.

References

- [1] An overview of freight vehicle wheel spalling / D. Day, R.F. Harder, M. Costello // Proceed-ings of 5th Int. Conf. on Railway Bogies and running gears. 2001. P. 229...237.
- [2] Contact fatigue damages of freight car wheels / Edited by S.M. Zakharov. Moscow: Inter-tekst. 2004. 160 p. (in Russian).
- [3] Increasing resistance of the railway wheels in operation by using carbonitride hardening of steel / L.M. Shkolnik, D.P. Markov, U.S. Proydak etc. // Herald of the Railway Research In-stitute (JSC VNIIZhT). 1994. No 6. P. 40...44. (in Russian).
- [4] A., Ekberg, Rolling contact fatigue of railway wheels // PhD Thesis Chalmers University of Technology. Gothenburg, Sweden. 2000. P. 1...27.
- [5] Effect of imperfections on fatigue initiation in railway wheels / A. Ekberg, J. Mareas // Jornal of Rail and Rapid Transit. 1999. P. 1...18.
- [6] Rolling contact fatigue of railway wheels under high axle load / P.J. Mutton, C.J. Epp, J. Dudec // Wear. 1997. Vol.211. P. 280...288.
- [7] On rolling contact fatigue analysis practice in railway industry: models and applications / J.D. Nast, C.L. Saux, B. Soua // Proceedings of 7th Int. Conf. on Railway Bogies and run-ning gears. 2007. P. 217...226.
- [8] A., Ekberg, Rolling contact fatigue of railway wheels – computer modeling and in-field data // Proceedings of 2nd mini conf. Contact mechanics and wear of rail/wheel systems. 1996. P. 154...163.
- [9] Tribology and its application on rail transport / Edited by D.P. Markov. Moscow: Intertekst. 2007. 408 p. (in Russian).
- [10] Sakalo A.V. Contact fatigue strength of railway wheel steel // Herald of the BSTU. 2011. №2. P. 35...41. (in Russian).
- [11] Reference book on strength of materials / Edited by G.S. Pisarenko. Kiev: Naukova dumka. 1988. 736 p. (in Russian).
- [12] A.A., Olshevsky, Methodology of solution of contact problems for bodies of arbitrary geometry with taking into consideration surface roughness by finite element method. PhD thesis, Bryansk, 2003. (in Russian).
- [13] Using of calculation schemes with reduced nodes at smoothing of finite element meshes / A.A. Burtsev, D.B. Titarev // Dynamics and strength of transport machines: collected sci-ence papers. Bryansk: BGTU. 2000. P. 44...49. (in Russian).
- [14] Application of super elements for solution of FEM problems with using of relaxation scheme of deformation / S.P. Novikov, V.I. Sakalo // Dynamics and strength of transport machines: collected science papers. Bryansk: BGTU. 2003. P. 43...48. (in Russian).
- [15] A.V., Sakalo, Method of simulation of contact stresses by using finite element fragments on elastic foundation // Herald of the VSTU. 2009. №9. P. 71...76. (in Russian).
- [16] O.C., Zienkiewicz, The finite element method in engineering science / London: McGraw-

- Hill. 1971. 521 p.
- [17] Contact problems of railway transport / V.I. Sakalo, V.S. Kossov. Moscow: Mashinostroenie. 2004. 496 p. (in Russian).
- [18] A fast, approximate method to calculate normal load at contact between wheel and rail and creep forces during rolling / W. Kik, J. Piotrowski // Proceedings of 2nd mini conf. Contact mechanics and wear of rail/wheel systems. 1996. P. 52...61.
- [19] J.J., Kalker, A Fast Algorithm for the Simplified Theory of Rolling Contact // Vehicle system dynamics. 1982. No 11. P. 1...13.
- [20] Theory of elasticity / S.P. Timoshenko, J.N. Goodier. New York: McGraw-Hill. 1970. 567 p.
- [21] K.L., Johnson, Contact mechanics / Cambridge University Press. 1985. 452 p.
- [22] A.V., Sakalo, Improvement of the railway wheel tread profile according to a contact fatigue criterion. PhD thesis, Moscow, 2011. (in Russian).